

# **Evolution of Cooperation under Environmental Variability**

Masaaki Inaba

March 2026

# **Evolution of Cooperation under Environmental Variability**

Graduate School of Science and Technology  
Degree Programs in Systems and Information Engineering  
University of Tsukuba

Masaaki Inaba

March 2026

# Abstract

[TODO]

# Contents

<b>Abstract</b>	i
<b>1 Introduction</b>	1
1.1 Theoretical background . . . . .	1
1.2 Environmental variability and modern human behavior . . . . .	3
1.3 Environmental variability and evolution of cooperation . . . . .	4
1.4 Research objectives and approach . . . . .	4
1.5 Organization . . . . .	5
<b>2 The base model</b>	7
2.1 Model . . . . .	7
2.2 Results . . . . .	12
<b>3 The 2-level model with migration</b>	19
3.1 Model . . . . .	19
3.2 Results . . . . .	25
<b>4 The 2-dimensional model with migration</b>	31
4.1 Model . . . . .	31
4.2 Results . . . . .	35
<b>5 Conclusion</b>	43
5.1 Summary of results . . . . .	43
5.2 Implications and interpretation . . . . .	43
5.3 Limitations and future directions . . . . .	44
<b>Appendix</b>	45
<b>Bibliography</b>	46
<b>Acknowledgments</b>	51

# List of Figures

2.1	Relationships, geographical structure, and EV.	9
2.2	The effect of RV.	12
2.3	The effect of UV.	13
2.4	The effect of CV ( $b = 1.8$ ).	14
2.5	Effects of EV on cooperation.	15
3.1	Illustration of the model structure.	20
3.2	Average cooperation rates as functions of $p_{EV}$ and $p_M$ .	25
3.3	Standard deviations corresponding to Figure 3.2.	26
3.4	Ablation experiments corresponding to Figure 3.2.	27
3.5	Temporal evolution of group-level cooperation.	28
3.6	Placeholder for Figure 3.6	28
3.7	Placeholder for Figure 3.7	29
3.8	Placeholder for Figure 3.8	29
3.9	Placeholder for Figure 3.9	30
4.1	Spatially heterogeneous prosperity patterns generated by SoR(s).	33
4.2	Influence of environmental variability ( $p_{EV}$ ) and agent mobility ( $p_M$ ) on the cooperation rate ( $\phi_C$ ).	36
4.3	Temporal dynamics under cyclic environmental variability.	37
4.4	Temporal dynamics under cyclic environmental variability with low agent mobility.	38
4.5	Influence of population size ( $N$ ) on cooperation rate ( $\phi_C$ ).	39
4.6	Temporal dynamics under cyclic environmental variability in the 1-SoR configuration.	41
4.7	Central resource-rich areas under $\phi_C^0 = 0.5$ or 1.0.	41
4.8	Influence of SoR orientation ( $p_{SoR}$ ) on the cooperation rate ( $\phi_C$ ).	42

# List of Tables

2.1	Model parameters used in the simulations.	11
3.1	Model parameters used in the simulations.	24
4.1	Model parameters used in the simulations.	35

# Chapter 1

## Introduction

Cooperation is fundamental to human society. Some forms of cooperation support basic biological survival and reproduction, including cooperative hunting, resource sharing, collective defense against predators, and alloparental care. Others reflect uniquely human sociality, such as division of labor, gift-giving, exchange, knowledge transmission, and formation of alliances. The prosperity of *Homo sapiens* would have been impossible without these behaviors. However, the evolutionary origins of cooperation are not fully understood and have been actively studied from Darwin's era to the present day.

### 1.1 Theoretical background

Darwin's theory of natural selection in *On the Origin of Species* (1859) [1] includes the principle that nature favors traits that increase individual fitness—the ability for individuals to survive and reproduce. However, although cooperative behaviors, particularly altruistic ones, appear to enhance the fitness of others or the group rather than the actor's own fitness, such behaviors are widespread across diverse taxa, from microorganisms to social insects to mammals. If nature favors a trait that increases individual fitness and cooperation decreases individual fitness, why is cooperation so ubiquitous? Darwin himself recognized this paradox [2].

This puzzle has been investigated first within evolutionary biology, and in later years across diverse disciplines including physics, economics, and psychology, collectively forming a research field known as the evolution of cooperation. In the following, we review several key studies in the evolution of cooperation, highlighting their main contributions and limitations.

Hamilton (1964) [3, 4] introduced the concept of inclusive fitness to explain the evolution of altruistic behaviors among genetically related individuals and formalized this insight as Hamilton's rule. This theoretical framework provides a powerful explanatory principle for cooperation among kin across diverse taxa, from social insects to primates. However, Hamilton's rule, in its original form, cannot explain altruistic behaviors between non-relatives, which are particularly prevalent in human societies. Recent attempts have been made to extend Hamilton's rule to

general cooperation mechanisms beyond kin relationships, but the validity of these extensions remains debated [5–7].

Maynard Smith and Price (1973) [8] introduced evolutionary game theory, providing a mathematical framework for analyzing how behavioral strategies, including cooperation and defection, spread in populations. Their approach treats strategies as heritable traits subject to natural selection, allowing researchers to predict which strategies will persist in populations over evolutionary time. This framework has become fundamental to studying the evolution of cooperation, as it enables formal analysis of how cooperative and selfish strategies compete and coexist.

Axelrod and Hamilton (1981) [9] demonstrated that reciprocal cooperation can evolve among non-relatives through repeated interactions. Using the iterated prisoner’s dilemma, they showed that simple reciprocal strategies such as Tit-for-Tat, which cooperates initially and then mimics the opponent’s previous action, can be evolutionarily successful, when individuals interact repeatedly and can recognize their past partners. This work established direct reciprocity as a fundamental mechanism for the evolution of cooperation. However, this mechanism requires individuals to recognize each other and remember past interactions, making it applicable primarily to small groups with repeated encounters. In large-scale societies where interactions are often anonymous or infrequent, alternative mechanisms are needed to explain the prevalence of cooperation.

Addressing these limitations, Nowak and his collaborators advanced research on various mechanisms that promote cooperation, including indirect reciprocity [10, 11], network reciprocity [12], and group selection [13]. Building on these studies, Nowak (2006) [14] synthesized the theoretical developments in the field, proposing five fundamental mechanisms for the evolution of cooperation: kin selection, direct reciprocity, indirect reciprocity, network reciprocity, and group selection. This framework provided a comprehensive taxonomy for understanding how cooperation can evolve under different ecological and social conditions. However, Nowak’s synthesis has been criticized as essentially reformulating Hamilton’s rule in different contexts, as each of these mechanisms can be understood within the framework of inclusive fitness theory [15]. Moreover, while this taxonomy is useful for categorizing mechanisms, it does not address how these mechanisms interact or which conditions favor one mechanism over another in realistic ecological settings.

These theoretical developments have established fundamental frameworks for understanding cooperation. We can no longer naively say that cooperation is a mystery. However, these frameworks remain highly general and abstract. Applying them to specific ecological and social contexts often requires additional assumptions about cognitive abilities, interaction structures, and environmental conditions. In recent years, research has increasingly shifted toward examining cooperation under more specific circumstances and mechanisms. These studies investigate how factors such as memory constraints, complex network structures, social norms, environ-

mental variability (EV), and learning mechanisms shape the evolution of cooperation. Such context-specific approaches complement the general theoretical frameworks and provide insights into the diverse forms of cooperation observed in nature and human societies. Among these context-specific factors, this dissertation focuses on EV.

## 1.2 Environmental variability and modern human behavior

Before examining how EV specifically affects cooperation, it is useful to consider a broader theoretical framework concerning the evolution of “modern human behavior”. In anthropology and archaeology, modern human behavior refers to a suite of traits characteristic of *Homo sapiens*, including abstract thinking, symbolic expression, complex planning, language, art, and crucially, large-scale cooperation and ultrasociality. Numerous studies concur that these behavioral patterns emerged during the Middle Stone Age (MSA) in Africa[16–20]. While there is broad consensus on when and where these behaviors originated, the mechanisms driving their emergence remain enigmatic, despite various proposed theories.

Among various hypotheses proposed to explain these developments, the variability selection hypothesis (VSH), proposed by Potts (1996, 1998) [21, 22], suggests that environmental unpredictability and variability was a primary driving force in human evolution. According to this hypothesis, intensified environmental fluctuations during MSA in Africa favored “versatilists” those capable of rapid adaptation to new environments over “specialists”, who adapt to specific environments, or “generalists”, who adapt across a range of environments. In this context, EV encompasses changes in landscape dynamics (such as land-lake oscillations), climate (such as arid-moist climate oscillations), variations in flora and fauna, ultimately leading to the unpredictability of resource availability.

Initially, this hypothesis was supported by a temporal correlation between intensified environmental changes, the replacement of human species, and the increased complexity of cultural artifacts, such as stone tools and ornaments [23]. In addition, the cognitive buffer hypothesis (CBH) [24–26] provides a neuroscientific basis for VSH, and a mathematical model [27] demonstrates its theoretical feasibility. The CBH posits that larger brain sizes in animals, including humans, evolved as a buffer against EV, enhancing survival through improved problem-solving and learning abilities. In contrast, several theories [28–30] propose that EV and behavioral diversity do not necessarily drive human encephalization. These theories emphasize the role of social contexts, as suggested by the social brain hypothesis (SBH) [23, 31–37], and consider other factors such as dietary influences [38, 39]. The SBH argues that human intellectual abilities evolved in response to the selection pressures of complex social environments, which required the effective management of social relationships within and between groups. There-

fore, while temporal correlations between EV and the behavioral innovations in hominins are evident, the causal mechanisms underlying these relationships remain unclear.

### 1.3 Environmental variability and evolution of cooperation

Large-scale and complex cooperation is also a key component of modern human behavior. We are interested in whether cooperation emerged in response to EV, as suggested by VSH for other behavioral traits.

[TODO: This paragraph is a temporary template and needs to be filled with actual literature review.] A growing body of research has examined the relationship between environmental variability and the evolution of cooperation. [TODO: Add specific studies from evolutionary biology]. [TODO: Add studies from physics/complex systems]. [TODO: Add studies from economics/game theory]. These studies have demonstrated [TODO: summarize key findings].

However, existing studies have primarily focused on [TODO: describe what existing studies examine]. In contrast, we hypothesize that [TODO: describe the specific type of EV relevant to MSA], characterized by [TODO: specific features], may have played a critical role in the evolution of large-scale cooperation during the MSA. This specific type of EV has not yet been systematically examined in the context of the evolution of cooperation.

Only a limited number of studies consider environmental factors in the evolution of cooperation, and these, typically in biological or physical contexts, focus on aspects such as extrinsic population variability [40, 41], variability in game structure [42, 43], variability in the strength of selection [44], the impact of EV on learning strategies [45], and resource pressure [46]. However, these studies do not fully address our research objective of understanding how EVs influences the evolution of cooperation.

### 1.4 Research objectives and approach

The key questions of this dissertation are: (i) Does EV promote the evolution of cooperation? (ii) If so, how does EV promote the evolution of cooperation?

As discussed earlier, EV during the MSA manifested through various interconnected fluctuations that collectively created unpredictable resource availability. These environmental fluctuations can be modeled in numerous ways. As a starting point, we consider three distinct approaches to modeling EV. We begin with a base model that examines the evolution of cooperation among spatially distinct groups. We then develop two extensions that incorporate migration between groups, a fundamental characteristic of pre-sedentary human populations. Each approach examines different aspects of how environmental conditions may have influenced

cooperation dynamics.

By answering these questions, we seek to understand whether the evolution of large-scale cooperation in humans can be explained, at least in part, by the variability selection framework.

Our study suggests that VSH, typically explained through the CBH, may also be connected to the SBH, which is generally considered separate from both VSH and CBH. While complex social environments encompass various factors, what uniquely characterizes human societies is the extensive and sophisticated cooperation observed, including intergroup cooperation and trade, which contrasts with the intragroup cooperation common in many animal societies. These advanced social behaviors are central to modern human behavior, and understanding their origins requires focusing on social factors that extend beyond individual-level adaptations, such as those proposed in CBH. Specifically, we demonstrate that EV fosters intergroup cooperation, which may have contributed to the development of complex social structures.

## 1.5 Organization

This chapter (Chapter 1) reviews the field of the evolution of cooperation, highlighting that while general theoretical frameworks have been well established, research examining cooperation under specific contexts remains an active area of investigation. We then introduce VSH, which proposes that EV drove the evolution of human behavior, including cooperation. Although temporal correlations between EV and behavioral innovations are evident, the causal mechanisms underlying these relationships remain unclear. Finally, we present the research objectives of this dissertation and describe three distinct approaches to modeling EV, each designed to examine different aspects of how EV may have influenced cooperation dynamics.

Chapter 2 introduces a base model that examines the evolution of cooperation among geographically distinct groups under EV. In this model, groups represent sites where resources may concentrate, such as riverbanks or lakeshores, where human populations naturally gathered. A limitation of this model is that it does not account for migration between groups.

Chapter 3 extends the base model by introducing a two-level structure with individual-level migration. Here, each geographical group, as defined in Chapter 2, contains multiple individuals who can move between groups. This framework allows us to examine how EV influences cooperation when individual migration is considered. However, while this model is a natural extension of Chapter 2, it represents a relatively unique approach within the existing studies on cooperation and migration, limiting comparability with prior works.

Chapter 4 addresses this limitation by employing a two-dimensional spatial structure, widely used in existing studies of cooperation with migration. In this model, without assuming explicit group structures, as defined in Chapters 2 and 3, we investigate how EV influences cooperation among individuals moving across a two-dimensional space.

Finally, Chapter 5 synthesizes the results from the three models in Chapters 2, 3, and 4 to

discuss how EV influences the evolution of cooperation. We further consider the implications and significance of this research, as well as its limitations and directions for future work.

# Chapter 2

## The base model

NOTE: This chapter is based on the following published paper and will be edited for the dissertation format. Currently, only the Model and Results sections have been inserted as placeholders.

Inaba, M., Akiyama, E., 2025. Environmental variability promotes the evolution of cooperation among geographically dispersed groups on dynamic networks. PLOS Complex Syst 2, e0000038. <https://doi.org/10.1371/journal.pcsy.0000038> [47]

In this chapter, we develop a foundational model that serves as the basis for the analyses in Chapters 3 and 4, with the aim of examining how environmental variability (EV) influence the evolution of cooperation.

### 2.1 Model

We use an agent-based simulation model within the framework of evolutionary game theory to investigate how increasing EV influences the evolution of cooperation. Given the limited availability of detailed data on EV and the spatial distribution of hominid groups during the MSA in Africa, our model adopts a highly abstracted approach, aiming to reveal the general effects of EV based on reasonable assumptions while excluding specific details. The model operates as follows: several geographically separated regions, each with varying levels of resource accessibility, experience fluctuating resource availability over time (EV). Each region hosts a single group (agent), and interactions between groups, such as resource exchanges (game) and behavioral pattern transmission (reformation), affect and adjust their relationships.

#### Agent and structure

In this model, each agent represents a single group and has a strategy of either cooperation or defection (in this study, "C" represents a cooperation strategy or a cooperator, while "D" represents a defection strategy or a defector). Initially, all agents are set to D, as intergroup

cooperation is considered extremely unlikely [48, 49]. This study focuses exclusively on intergroup interactions and does not consider intragroup interactions. While a two-level model would be necessary to analyze the tension between intergroup and intragroup interactions, as seen in multilevel selection studies, a one-level model is suitable here given our focus on intergroup interactions. All agents are suited within a geographic structure, forming an interaction structure.

The geographic structure is modeled as a line segment with periodic boundary conditions, represented visually as a circle (Fig 2.1).  $N$  agents are evenly spaced along the circle. Although a one-dimensional spatial structure is used for simplicity, more realistic structures can be explored as empirical studies progress. Mobility is not considered in this study to keep the model simple as an initial approach. We plan to incorporate mobility in future work, as it is reasonable to assume that a group might move to a resource-rich region when its resources become scarce. However, the assumption of no mobility is not entirely unrealistic, as some studies have highlighted the tendency for settlement during the MSA [50–52].

The interaction structure defines the relationships between agents, which are not limited by the geographic arrangement. These relationships affect the frequency of games (described later) and are subject to rewiring through reformations (also described later). The network, where agents are represented as nodes and relationships as edges, is characterized as an undirected, unweighted, and dynamic graph. The initial network is a regular network with a degree of  $k = 4$ .

## EV

The resource represents the amount of goods or wealth necessary for survival that a group (agent) can obtain from the natural environment (e.g., food, materials for stone tools required to gather food). Resources are allocated to each agent at each time step, with the amount varying across different regions. The node with the highest resource allocation is referred to as the source of resources (SoR). The further an agent is located from the SoR geographically, the less resource it receives, as determined by the resource decrement factor,  $f_{RD}$ . Specifically, the resource allocated to agent  $i$  is calculated as  $r_i = r_p - |i - p|f_{RD}$ . Here,  $r_i$  represents the resource allocated to agent  $i$ ,  $p$  is the index of the SoR, and  $|i - p|$  represents the distance between  $i$  and  $p$ , accounting for the boundary conditions, rather than the usual absolute value. Additionally, there is a universal resource threshold,  $\theta$ , for all agents; any agent falling below this threshold must reformulate its strategy and relationships.

In our study, EV refers to resource variability, represented by stochastic models. EV can be divided into variability in distribution of resources among regions and in total quantity of resources across all regions. Although variations in resource types are also an important consideration, we simplify the model assuming a single resource type. The two forms of vari-

ability are termed regional variability (RV) and universal variability (UV). RV is a type of EV in which the distribution of resource-rich and resource-poor regions changes over time; specifically, the SoR moves randomly. The SoR's index  $p_t$  at time  $t$  fluctuates according to a stochastic process expressed as  $p_{t+1} = (p_t + \Delta_t) \bmod N$ . Here,  $\Delta_t$  is a random integer step uniformly distributed within the range  $[-\sigma_R, \sigma_R]$ , where  $0 \leq \sigma_R \leq N/2$ . UV represents another form of EV in which the total resource quantity fluctuates randomly over time, while the resource distribution between regions remains fixed. This variability reflects large-scale fluctuations in resource availability across a wide area encompassing all regions. However, to simplify the implementation, we fix the resource values and instead model UV by varying the threshold value  $\theta$ , which determines when reformation occurs. The fluctuation is modeled by an AR(1) process [53–55],  $\theta_{t+1} = \mu_\theta(1 - \beta) + \theta_t\beta + \epsilon$ , where  $\mu_\theta$  is the expected value of  $\theta$ ,  $\beta$  is the autoregressive coefficient ( $0 \leq \beta \leq 1$ ), and  $\epsilon$  is a normally distributed noise term with mean 0 and standard deviation (SD)  $\sigma_\theta$ . The intensity of RV is determined by the shift range of the SoR ( $\sigma_R$ ), while the intensity of UV is influenced by the autoregressive coefficient ( $\beta$ ) and the SD of the noise term ( $\sigma_\theta$ ). We examine the impact of EV on the evolution of cooperation under three scenarios: RV, UV, and combined variability (CV), where both the SoR shifts and the threshold  $\theta$  fluctuates.

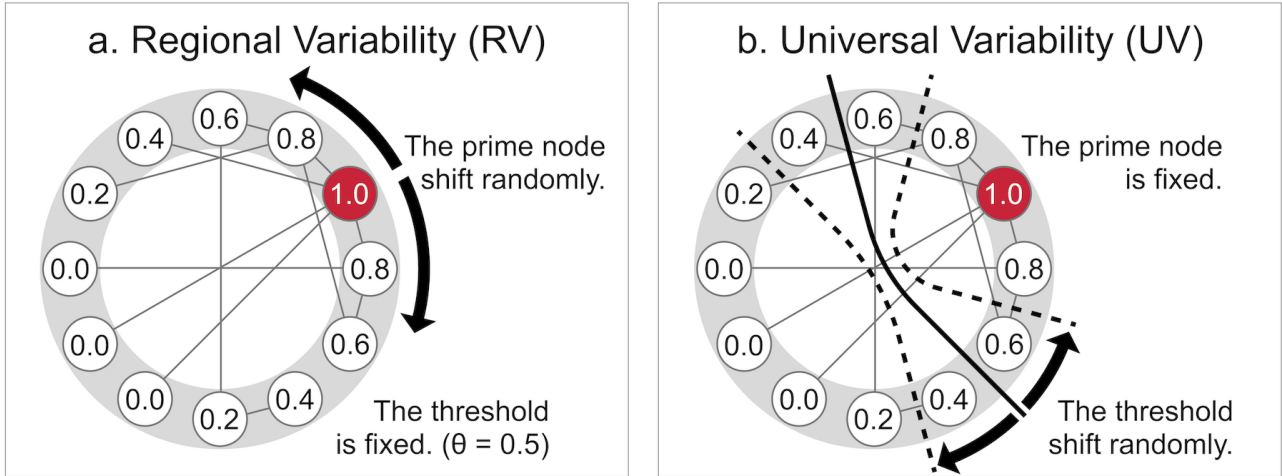


Figure 2.1: Relationships, geographical structure, and EV. Each small circle within the gray circle represents a group (agent, node), with the number inside indicating the resource value. The gray ring represents the geographical structure, and each line connecting agents denotes a relationship (edge). (a) In the RV model, the SoR shifts randomly within the geographical structure, and resources are then allocated to other nodes. Following this, the game and reformation processes occur. The resource threshold for reformation is fixed at  $\theta = 0.5$ . (b) In the UV model, the SoR remains fixed, but the threshold  $\theta$  fluctuates randomly, following an AR(1) process.

## Game

Communication over resources (such as primitive bartering, giving, looting) between agents is represented by simple pairwise games. These games can only be played with an opponent who is connected through a network edge. The probability that agent  $i$  selects agent  $j$  as its game opponent from its neighbors is  $p_{i,j}^G = \frac{1}{n}$ ;  $n$  is the number of neighbors of  $i$ , and neighbors refer to an agent directly connected to  $i$  in the interaction structure network. The game procedure follows a pairwise public goods game (PGG) [56–59] with resource threshold considerations. First, assume that agent  $i$  selects agent  $j$ . If the agent is C, it contributes a surplus resource  $M_i = \max(r_i - \theta, 0)$ . If the agent is D, it does not contribute any resource. The contributed resources are multiplied by a factor  $b$  ( $1 \leq b \leq 2$ ) and then equally divided between  $i$  and  $j$ . The payoff table is as follows:

	$C$	$D$
$C$	$R_i, R_j$	$S_i, T_j$
$D$	$T_i, S_j$	$P_i, P_j$

(2.1)

$$R_i = \left(\frac{b}{2} - 1\right) M_i + \frac{b}{2} M_j \quad (2.2)$$

$$S_i = \left(\frac{b}{2} - 1\right) M_i \quad (2.3)$$

$$T_i = \frac{b}{2} M_j \quad (2.4)$$

$$P_i = 0 \quad (2.5)$$

The social optimum, which maximizes the sum of both payoffs, is CC under  $b > 1$ . The Nash equilibrium is when DD for  $b < 2$ . Thus, a social dilemma exists across the defined range of  $b$ , except at the boundaries. Additionally, by solving  $T_i > R_i > P_i > S_i$ , the condition for the game to qualify as a prisoner's dilemma is  $b > 1 + \frac{M_i - M_j}{M_i + M_j}$ . If this condition is not met, then  $T_i > P_i > R_i > S_i$ .

We have chosen this game model instead of classic pairwise games to implement the condition that only agents with surplus resources can contribute to other agents. In classic pairwise games, such as the prisoner's dilemma or the snowdrift game, benefits and costs are fixed at constant values. This implies that agents would cooperate identically, regardless of resource abundance or scarcity, even under uncertain survival conditions. This assumption is inconsistent with our research context. Therefore, we have developed and adopted a novel pairwise PGG model that accounts for resource availability.

## Reformation

If, as a result of the games, an agent's resource falls below the threshold  $\theta$ , it is considered to have failed to adapt to the environment, triggering a reformation of its strategy and network connections. An agent  $i$  that falls below  $\theta$  randomly selects a role model. The probability that  $j$  is chosen as its role model is  $p_j^R = \frac{r_j}{\sum_{k \in [1, \dots, N]} r_k}$ . The  $i$  imitates  $j$ 's strategy, with mutation occurring at a probability  $\mu$ . Additionally, agents that fall below the threshold disconnect all of their current relationships. They then randomly select the same number of new neighbors as the number of disconnections and establish new connections. The probability that agent  $j$  is chosen as a new neighbor is proportional to  $p_j^R$ . In other words, the higher the resource, the more likely an agent is to be chosen as a role model and a new neighbor.

## Evaluation

The simulation runs for 10,000 generations, with 100 independent simulations conducted for each parameter set (Table 2.1). Resource allocation and interactions, including games and reformations, occur once per generation. The proportion of agents employing strategy C in each generation is referred to as the cooperation rate. The average cooperation rate is calculated as the mean of the cooperation rates across trials, considering only the last 50% of the generations. To assess the effect of EV on the evolution of cooperation we compared the average cooperation rates across different parameters controlling RV and UV, along with other factors.

The effect of EV was assessed by comparing the average cooperation rates across various parameters.

Parameter	Description	Value
$N$	Number of agents	100
$n_0^C$	Initial number of C agents	0
$k_0$	Initial degree of the interaction structure network	4
$t_{max}$	Number of time steps (generations) for a simulation	10,000
$trials$	Number of simulations per parameter set	100
$r_{max}$	Max resource	1.0
$f_{RD}$	Resource decrement factor	0.02
$\sigma_R$	Shift range of the SoR	$\{0, 1, \dots, 49\}$
$\mu_\theta$	Expected value of threshold $\theta$	0.5
$\beta$	Autoregressive coefficient of the UV	$\{0.0, 0.1, \dots, 0.9\}$
$\sigma_\theta$	SD of the noise term of UV	$\{0.0, 0.1, 0.2\}$
$b$	Multiplication factor for PGG	$\{1.0, 1.1, \dots, 2.0\}$
$\mu$	Mutation rate for strategy imitation	0.01

Table 2.1: Model parameters used in the simulations.

## 2.2 Results

### Effect of RV

We first examined the impact of RV in isolation, without considering UV. Specifically, in each generation, the SoR randomly shifts within the range of  $[-\sigma_R, \sigma_R]$ , accounting for the periodic boundary condition. The threshold  $\theta$ , which universally affects the resource welfare of all agents, is fixed at 0.5.

The results (Fig 2.2a) suggest that RV can promote the evolution of cooperation. To elaborate, when the SoR is fixed ( $\sigma_R = 0$ ), cooperation does not evolve. As variability slightly increases ( $\sigma_R = 1$ ), the cooperation rate rises to around 10%. For  $b \leq 1.7$ , further increases in variability do not promote additional cooperation, although the cooperation rate remains higher than when  $\sigma_R = 0$  or 1. However, for  $b \geq 1.8$ , greater variability further enhances cooperation.

Despite the overall positive effect of higher variability on cooperation, cooperation is not completely stable and fluctuates with temporary environmental changes. For example, when  $b = 1.8$  and  $\sigma_R \in [1, 4, 16]$ , the temporal transition (Fig 2.2b) shows that the cooperation rate rises and falls dramatically.

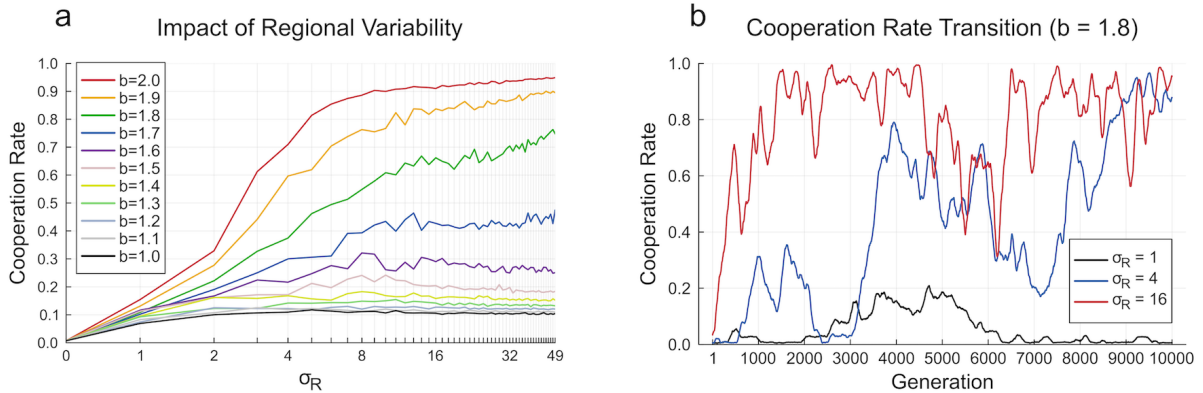


Figure 2.2: The effect of RV. (a) The effect of RV across  $b \in [1.0, \dots, 2.0]$ . The horizontal axis represents the intensity of RV,  $\sigma_R$ , and the vertical axis shows the mean cooperation rate over the last 5,000 generations, averaged across 100 trials. (b) Examples of cooperation rate transitions when  $b = 1.8$  and  $\sigma_R \in [1, 4, 16]$ . The horizontal axis represents generations, and the vertical axis shows the cooperation rate. Higher RV tends to result in fluctuations of the cooperation rate at higher levels, though convergence is not observed.

### Effect of UV

Next, we examined the effects of UV while excluding RV. As previously defined, UV refers to fluctuations in the threshold  $\theta$  across generations, which uniformly affects all agents. The intensity of this variability is controlled by the autoregressive coefficient  $\beta$  and the SD  $\sigma_\theta$  of the

noise term in the AR(1) stochastic model. With the SoR fixed at  $p = 1$ , resources are allocated less as the distance from this node increases.

We found that while UV promotes the evolution of cooperation to some extent, its effect is considerably more limited than that of RV. For  $\sigma_\theta = 0.1$ , the cooperation rate gradually increases when  $\beta$  exceeds 0.5, but it peaks at just 30% (Fig 2.3a). For  $\sigma_\theta = 0.2$ , the cooperation rate remains between 20% and 30%, regardless of  $\beta$ , and increasing variability further does not affect these outcomes (Fig 2.3a).

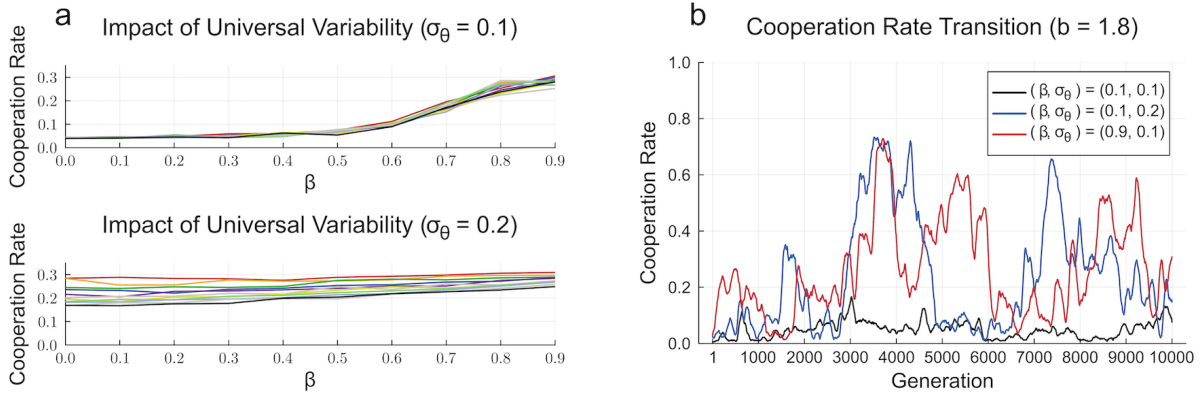


Figure 2.3: The effect of UV. (a) The effect of UV across  $b \in [1.0, \dots, 2.0]$  and  $\sigma_\theta \in [0.1, 0.2]$ . The horizontal axis represents the intensity of UV,  $\beta$ , and the vertical axis shows the mean cooperation rate over the last 5,000 generations across 100 trials. (The line color scheme of these lines is same as in Fig 2.2a.) (b) Examples of the cooperation rate transition when  $b = 1.8$  and  $(\beta, \sigma_\theta) \in [(0.1, 0.1), (0.1, 0.2), (0.9, 0.1)]$ . The horizontal axis represents generations, and the vertical axis shows the cooperation rate. Higher UV tends to result in the cooperation rate fluctuating at higher levels, but convergence is not observed.

## Effect of CV

We then examined the combined effects of both RV and UV. The results (Fig 2.4) show that, consistent with the separate analyses above, RV strongly promotes the evolution of cooperation, while UV has much subtle effect.

## Primary drivers of the results

The results are driven by two key factors: 1. the effects of mutation and EV, which promote fluctuations in cooperation rates, and 2. the coevolution of cooperation and network structure.

First, RV increases the fluctuations in the cooperation rate, rather than the rate itself. Fig 2.5a shows the effect of EV on strategy distribution in a model that entirely excludes the effects of games and networks. When these effects are excluded, changes in strategy distribution occur solely due to mutation and strategy updating. The Y-axis represents the number of agents generated by mutation in one generation, who then serve as role models for strategy updating

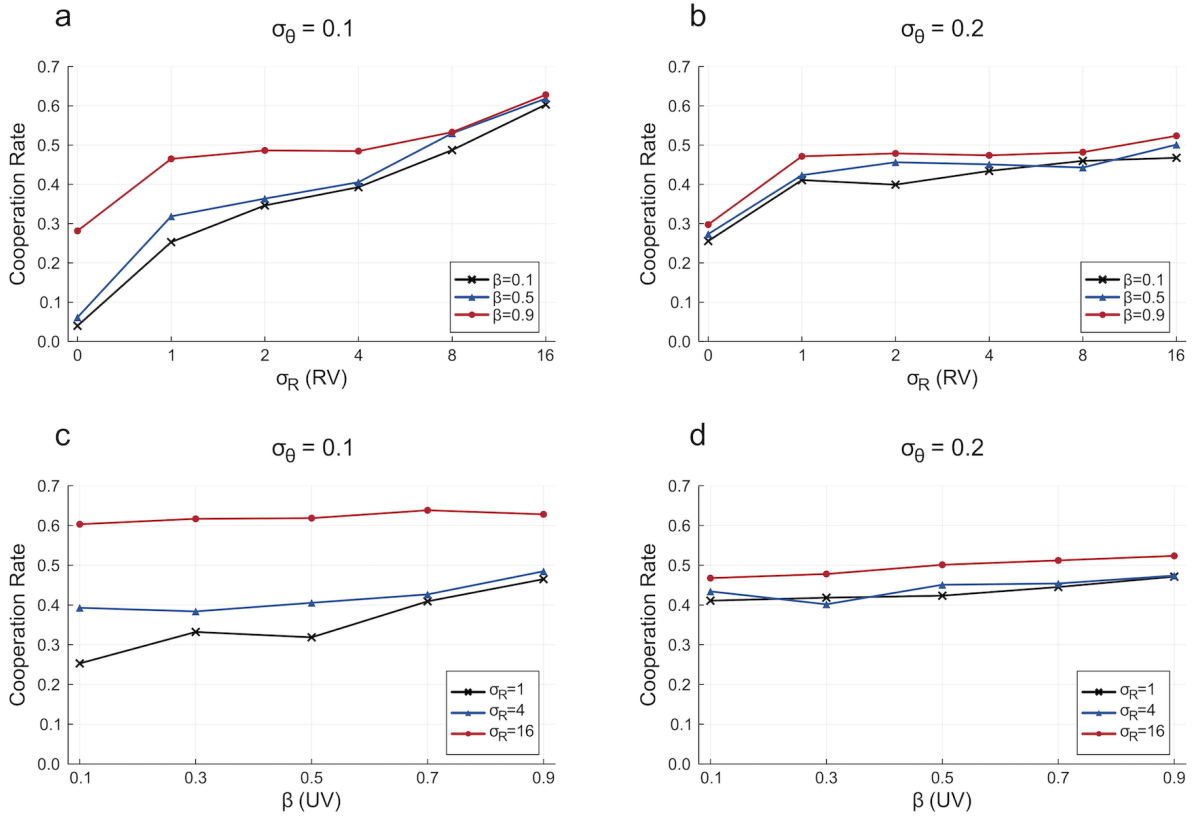


Figure 2.4: The effect of CV ( $b = 1.8$ ). (a) and (b) represent cases with  $\sigma_\theta = 0.1$ , each with a different x-axis. These plots show that RV increases the cooperation rate significantly, while UV has a limited effect. (c) and (d) represent cases with  $\sigma_\theta = 0.2$ , with different x-axis. The lines are almost flat except in the range  $\sigma_R = 0$  to 1, indicating that when UV is too high, not only UV but even RV has no effect on the cooperation rate.

in the next generation. These agents are the source of changes in strategy distribution. The line for RV in the figure shows that as the variability increases, the number of mutated role models increases linearly. Fig 2.5b “3. (env, C rate)” shows that the time series of RV and the cooperation rate in each of the 100 trials are completely uncorrelated. Furthermore, the results remain unchanged even when cross-correlation analysis is performed, accounting for time delays. Therefore, it is evident that RV does not directly affect the cooperation rate but instead promote fluctuations in it. This can be explained as follows: agents in poorer regions frequently undergo reformations and mutations. When RV is small, agents rarely accumulate resources in the next generation, causing them to undergo reformations again. However, when variability is large, agents may become resource-rich in the next generation, and they potentially survive to influence the strategy updates of other agents. When RV is large, the cooperation rate is more likely to fluctuate up and down.

Notably, the analytical solution (2.6) aligns closely with the simulation results for RV shown

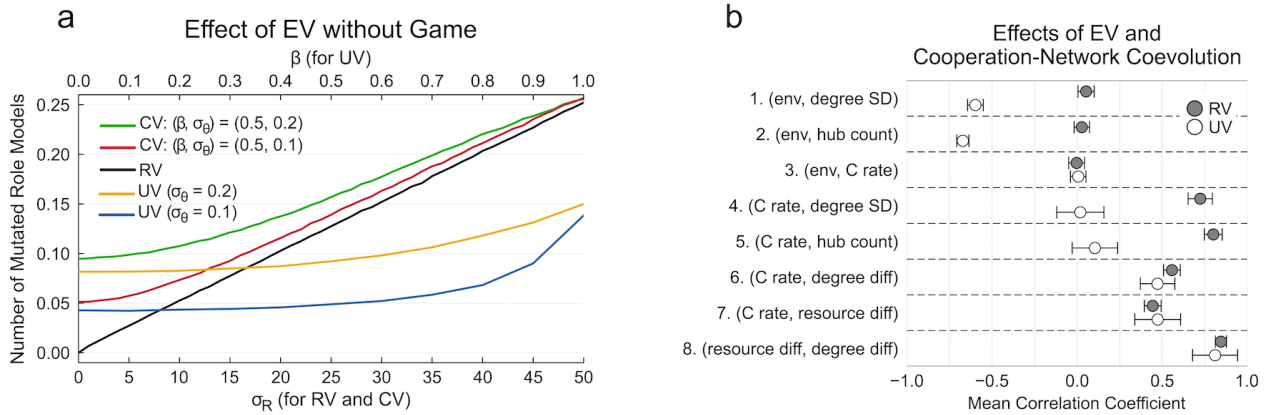


Figure 2.5: Effects of EV on cooperation. (a) The number of mutated role models as a function of RV and UV. The simulations are based on a model that excludes games. Therefore, the figure shows how EV and reformation impact the system without the effect of games or network structure. (b) Correlation analysis through time series (10,000 generations) between variables related to EV (For RV, env refers to the shift distance of the SoR per generation; for UV, env refers to the value of threshold  $\theta$ ), network structure (degree SD: standard deviation of degrees, hub count: number of nodes with a degree of 10 or more), and cooperation (C rate: frequency of C, resource diff: the difference in average resources between C and D, and degree diff: the difference in average degree between C and D). The mean correlation coefficients are averaged over 100 trials for both RV and UV.  $b = 1.8$  for all simulations,  $\sigma_R = 16$  for RV, and  $\beta = 0.7$ ,  $\sigma_\theta = 0.1$  for UV.

in Fig 2.5a.

$$\begin{aligned} E[n_{MR}] &= \sum_{k=0}^n \mu^k (1-\mu)^{n-k} k \frac{\sigma_R}{N} \\ &= \frac{n\mu}{N} \sigma_R \end{aligned} \quad (2.6)$$

In this equation,  $E[n_{MR}]$  denotes the expected number of mutated role models, which are generated through mutation and later serve as role models for the strategy updates of other agents. The right-hand side of the equation represents the expected number of mutated agents within a population of reformed agents,  $n$ , weighted by the effect of RV,  $\sigma_R$ , across the entire agent population,  $N$ . This equation is simplified by applying the formula for the expectation of a binomial distribution.

Second, once the cooperation rate increases, it is likely sustained through the coevolution of cooperation and network structure. Fig 2.5b 7 indicates that the cooperation rate is correlated with the difference in resources between C and D. This correlation likely arises because, as the frequency of C increases, mutual support among Cs strengthens, leading to an increase in the average resources of C. Fig 2.5b 8 further shows that the difference in resources is strongly correlated with the difference in network degree between C and D. This occurs because, in the reformation process of our model, agents with more resources acquire more edges. Finally, Fig 2.5b 6 demonstrates that there is a correlation between the difference in degree and the

cooperation rate. This is likely because, as shown in several studies [59–61], heterogeneous degree distributions tend to facilitate cooperation in networks. Thus, a positive feedback loop can form, in which an increase in the cooperation rate induces resource heterogeneity, which subsequently results in network degree heterogeneity, and this network heterogeneity, in turn, reinforces the cooperation rate, which is thought to help sustain the maintenance of a cooperation rate that initially emerged by chance. This explanation is based on correlation and inference, and does not rule out the involvement of other factors. One possible factor is the influence of resource heterogeneity on strategy update frequency, which has been suggested to promote cooperation [62]. This process may operate alongside the previously described process where an increase in the cooperation rate widens the resource gap between C and D.

In contrast, UV does not significantly promote cooperation for two reasons: it fails to generate sufficient fluctuation in the cooperation rate, and it inhibits the coevolution of cooperation and the network structure. As shown by the two UV lines in Fig 2.5a, increasing variability does not substantially increase the number of mutated role models, unlike the linear relationship seen with RV. Furthermore, when UV is intense and the threshold  $\theta$  becomes very large, almost all agents undergo reformation. This leads to a reduction in network heterogeneity, which is critical for the coevolution of cooperation and network structure. This is reflected by the strong inverse correlation between UV and network heterogeneity (Fig 2.5b 1-2). The factors that promote cooperation in RV are ineffective in the context of UV, which explains why UV does not significantly promote cooperation. When RV and UV are combined in the CV model, the results remain consistent, RV promotes cooperation, while UV has a much smaller effect.

In summary, the observed patterns in cooperation rates can be attributed to the combined effects of mutation and EV, as well as the coevolution of cooperation and network structure. Specifically, when these two factors work well together, as in the RV model, environmental change promotes cooperation. However, when the first factor is weak and inhibits the second, as in the UV model, cooperation is less likely to evolve.

## Discussion

Building on Potts's VSH [21, 22], we explored the effects of EV through two simplified models: RV and UV models. Our results show that RV clearly promotes the evolution of cooperation, while UV has a much smaller effect. The reason RV fosters cooperation is that it disrupts the distribution of strategies, and the cooperative states that occasionally emerge from these disturbances are sustained by the coevolution of cooperation and network structure. In contrast, UV does not significantly promote cooperation because the disturbances it causes are insufficient and because it hinders the evolution of the network structure. Even when both RV and UV are combined, only RV proves effective, with UV having little impact. Thus, when EV's dis-

turbance effect and the coevolution of cooperation and network structure align, EV facilitates the evolution of cooperation. However, EV does not promote cooperation if it fails to create sufficient disturbance in strategy distribution or if it undermines the network's heterogeneous structure.

Our study offers a new perspective on the evolution of cooperation and has the potential to guide future research on modern human behavior in archaeological contexts. First, although some research on the evolution of cooperation considering EV has been conducted in biology and physics [40–44], few studies have approached it from an anthropological perspective. To address this gap, we offer a novel explanation for how EV may influence cooperative behavior, using a model that simulates interactions among human groups during the MSA. Notably, we also identify a key condition for EV to promote cooperation: cooperation and network structure must coevolve effectively. Second, our findings suggest that the VSH, which has primarily been linked to the CBH, may also be connected to the SBH, thus expanding the scope of VSH. The conventional CBH explanation [21, 22, 24–26] is that the brains of the “versatilists,” evolved to rapidly adapt to new environments under EV, contributing to the development of modern human behavior. In contrast, our novel interpretation, linking EV to SBH, suggests the following sequence. EV promotes intergroup cooperation, as demonstrated in our study. The cooperation likely leads to the emergence of more complex, interdependent societies, which introduce new social challenges such as communication, coordination, and conflict resolution across group boundaries. The increasing complexities of these societies exerts selection pressure on cognitive abilities, favoring individuals who are better equipped to navigate these dynamics. Over time, this process likely drives the evolution of modern human behavior, characterized by advanced intellectual abilities and complex social structures. Finally, not previously mentioned, our network model, which incorporates both relationship and geographical structures, can be viewed as a type of multiplex network [63]. This perspective opens new avenues for mutual enrichment by enabling comparisons between our findings and the extensive body of research on multiplex and multilayer networks [63–66], potentially providing deeper insights into the dynamics of cooperation within complex social and spatial frameworks.

Although this study provides valuable insights into the relationship between EV and cooperation, several limitations should be considered for a more comprehensive understanding. These limitations include the validity of our model in relation to real-world scenarios during the MSA, the extent to which our results explain actuality, and the need for further mathematical analysis. We have prioritized simplicity in constructing the model; it is essential to verify which aspects align with reality and which do not. This includes evaluating the EV patterns, geographical structure, population and grouping dynamics, the specifics of intergroup interactions (game), and the mechanisms through which collective behaviors propagate (reformation), as influenced by empirical research. An important aspect of intergroup interactions that our current model does not account for is an interaction model biased by the memory of past cooperation and ex-

ploitation. This extension, which assumes that agents interact more frequently with those who have previously cooperated with them while avoiding those who have not, could provide insights into the emergence of more complex social structures. Meanwhile, as our model focuses on the effects of resource variability, neighbor selection is driven by resource availability. However, in reality, the network is also shaped by exogenous and random factors. Models incorporating such factors, known as temporal networks [67–69], have received growing attention. Future extensions accounting for these factors may provide new insights and broaden our research scope. Additionally, population changes and mobility must be considered, and we plan to address mobility in future work. We also need to wait for future empirical studies to assess how well our results correspond to the actual events of the MSA. Furthermore, mathematical analysis is required to better understand the conditions under which EV and other dynamic structures can foster cooperation. Although the complexity of the phenomenon makes it challenging to propose analytical solutions, theoretical research using simpler models should complement our findings. Thus, while our study does not aim to establish universal laws, it presents a valuable hypothesis that is expected to guide future theoretical and empirical research in this area.

# Chapter 3

## The 2-level model with migration

**NOTE:** This chapter is based on an ongoing manuscript. The Model section is approximately 80% complete, and the Results section is approximately 50% complete. Both sections will be finalized and integrated into the dissertation structure.

### 3.1 Model

This model is designed to explore the effects of environmental variability and agent mobility on the evolution of cooperation.

#### Agent, group and structure

We consider the model composed of multiple regional groups, each inhabited by a number of humans who may migrate between the groups in response to environmental or social pressures. Within this world, the population is represented by agents and regional groups, and their interaction (see Subsection 3.1) and migration (see Subsection 3.1) are governed by the geographical and interaction structures (see Figure 3.1).

In this model, there are  $n_F$  agents and  $n_R$  regional groups. An agent is an abstract representation of the minimal unit of human migration, such as a family. A group represents the set of agents within a geographically dispersed human habitat.

The geographical structure constrains the positions of groups and the migration of agents. It is defined as a circular graph, i.e., a ring structure, in which each group is connected to its two neighboring groups. These connections remain fixed throughout the simulation. The agents are initially distributed evenly across all groups and can migrate between neighboring groups during the simulation. The migration results in uneven spatial distributions of agents over time, and some groups can be empty.

The interaction structures constrain the selection of opponents for cooperative or competitive interactions at two levels, i.e., inter-group and intra-group (between agents). There is

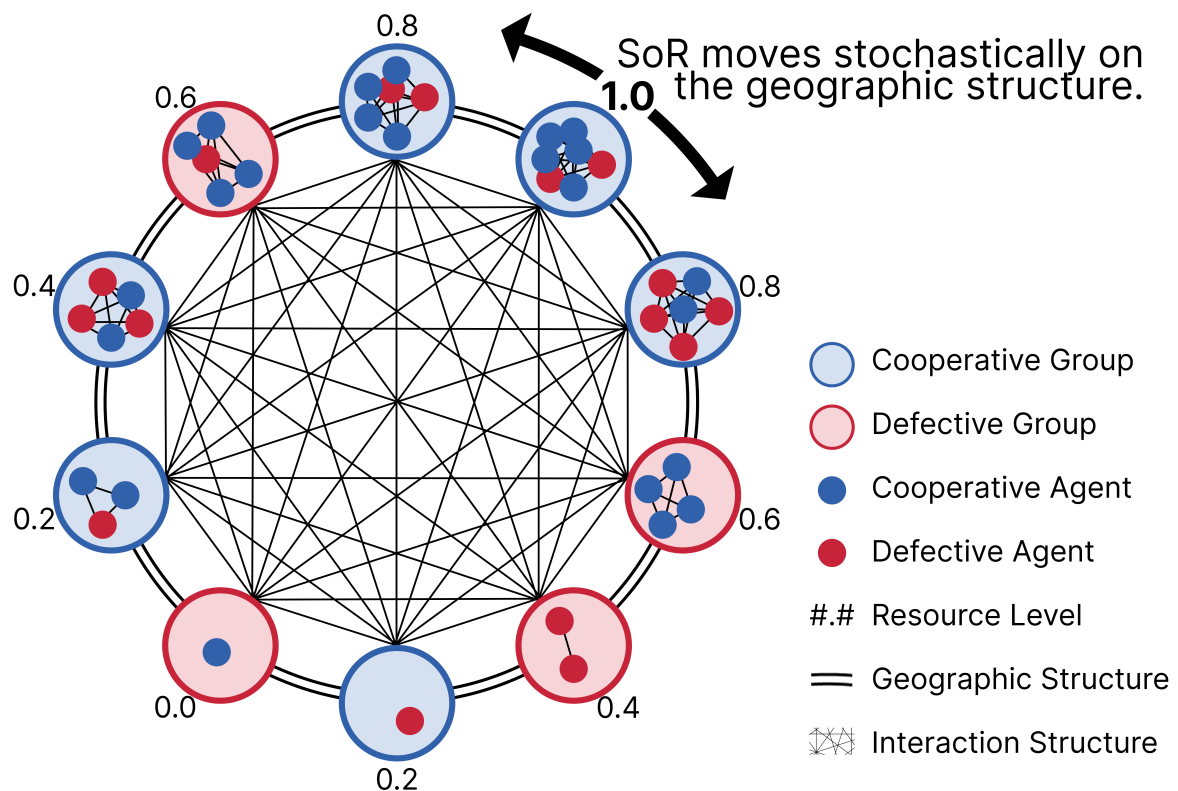


Figure 3.1: Illustration of the model structure. Regional groups are arranged on a circular geographic structure, where the SoR stochastically moves between groups. Each group contains agents. Each group and each agent independently adopt either  $C$  (blue) or  $D$  (red). Numbers indicate group resource levels, which decrease with distance from the SoR. Interaction structures exist at the group level and at the agent level within each group.

a single inter-group interaction structure in the model, while each group has its own intra-group interaction structure and no interactions occur between agents belonging to different groups. An interaction structure is represented by a weighted, undirected, complete graph whose edge weights are dynamic while its topology remains fixed. The dynamic edge weight  $w_{i,j}$  ( $0 \leq w_{i,j} \leq 1$ , initialized at  $w_0$ ) denotes the strength of the relationship between nodes  $i$  and  $j$ , where a node represents either a group or an agent, and is proportional to the probability of interaction between them.

Given these structural foundations, the simulation proceeds in four stages: environmental variability, game, migration, and strategy update. Game and strategy updates occur at both the group and agent levels, in that order. Each stage is described in the following subsections.

## Environmental variability

The model captures a key feature of the environmental variability observed during the MSA in Africa, namely the unpredictable shifts in the geographical distribution of resources.

To represent this type of variability, we define the source of resources (SoR) as a dynamic point corresponding to the most resource-abundant region. The SoR moves stochastically across the regional groups introduced in Subsection 3.1 at each simulation time step. This stochastic movement is formalized as

$$x_{t+1} = \begin{cases} [(x_t + \Delta_t - 1) \bmod n_R] + 1, & \text{with probability } p_{EV}, \\ x_t, & \text{otherwise,} \end{cases} \quad (3.1)$$

where  $x_t$  denotes the index on the circular graph of regional groups indicating the position of the SoR at time  $t$ ,  $\Delta_t \in \{-1, +1\}$  is chosen with equal probability, and  $p_{EV}$  is a key parameter controlling the intensity of the environmental variability.

The group at which the SoR is located receives a resource value of 1. The amount of resources allocated to other groups decreases with their distance from the SoR along the geographical structure, reaching 0 for the group farthest from the SoR. This resource allocation is formalized as

$$r_i^R = 1 - \frac{d_i}{\left\lfloor \frac{n_R}{2} \right\rfloor} \quad (3.2)$$

where  $r_i^R$  denotes the resources received by group  $i$ , and  $d_i$  is the distance between group  $i$  and the SoR, calculated with periodic boundary conditions. The resources of each group are evenly shared among its agents.

## Game

Interactions that affect gains and losses of resources, both between groups and between agents, are modeled using a game-theoretic framework. Because interactions at the group and agent levels often follow the same rules, we occasionally use the term *entity* as a general label for both. Entity  $i$  adopts a strategy  $s_i \in \{C, D\}$ , where  $C$  denotes cooperation and  $D$  denotes defection. The interaction dynamics consist of three sequential phases: opponent selection, a pairwise public goods game (PGG), and an update of the interaction structure.

The opponent selection is based on the relationships between entities specified by the edge weights of the interaction structure. Each entity  $i$  stochastically selects another entity as its opponent, with the probability of selecting entity  $j$  given by

$$P(j|i) = \frac{w_{i,j}}{\sum_{k \neq i} w_{i,k}}. \quad (3.3)$$

Each selected pair then engages in a pairwise PGG. Here, we employ a pairwise PGG rather than traditional pairwise games such as the Prisoner's Dilemma Game and the Stag Hunt Game in order to incorporate both the resource value of each entity and the relationships into the game. In the game between entity  $i$  and  $j$ , both contribute their respective amounts  $c_i$  and  $c_j$ ; the total contribution is multiplied by a constant factor  $b$ , and the amplified resources are then shared equally between them. Specifically,  $c_i$  is defined as

$$c_i = \begin{cases} r_i \times w_{i,j}, & \text{if } s_i = C, \\ 0, & \text{if } s_i = D \end{cases} \quad (3.4)$$

where  $r_i$  denotes the resource available to entity  $i$  at the time of the game. In summary, the payoff matrix for entities  $i$  and  $j$  is

		$C$	$D$
$C$	$\frac{(c_i+c_j)b}{2} - c_i, \frac{(c_i+c_j)b}{2} - c_j$	$\frac{c_i b}{2} - c_i, \frac{c_j b}{2}$	
$D$	$\frac{c_i b}{2}, \frac{c_j b}{2} - c_j$	$0, 0$	

(3.5)

Finally, the edge weights of the interaction structure are updated to reflect the outcomes of the pairwise games. Because entities benefit from being connected to  $C$  but not to  $D$ , the direction of change depends on the combination of strategies. When  $C-C$ , each has an incentive to strengthen the tie, and the relationship becomes stronger. When  $C-D$  or  $D-C$ , one side tends to strengthen while the other tends to weaken the tie; these opposing tendencies cancel out, and the relationship remains unchanged. When  $D-D$ , each has an incentive to weaken the tie, and the relationship becomes weaker. Formally, the update of the edge weights is given by

$$w'_{i,j} = w_{i,j} + (T - w_{i,j})\Delta w, \quad (3.6)$$

where  $\Delta w$  ( $0 \leq \Delta w \leq 1$ ) denotes the update rate, and the target value  $T$  is set to 1 if  $C-C$ ,  $w_{i,j}$  if  $C-D$  or  $D-C$ , and 0 if  $D-D$ .

## Migration

Agents facing resource scarcity stochastically migrate to an adjacent regional group in search of better conditions. Specifically, the probability that migration occurs is given by

$$\max\left(1 - \frac{r_i^F}{\theta_F}, 0\right) \cdot p_M, \quad (3.7)$$

where  $r_i^F$  denotes the resource available to agent  $i$ ,  $\theta_R$  ( $0 < \theta_R < 1$ ) is the universal threshold shared by all groups,  $\theta_F$  is the per-agent threshold obtained by  $\theta_F = \frac{\theta_R}{n_F/n_R}$ , and  $p_M$  is a parameter controlling the frequency of migration events.

The migration direction is also probabilistic: with probability  $p_{SoR}$ , the agent moves to the neighboring group closer to the SoR; otherwise, it chooses randomly between the two neighboring groups.

Upon migration, the agent establishes new relationships in the destination group, and discards all previous ones. Specifically, the edge weights between the agent and the others in the destination group are set to  $w_0$ , and the edge weights between the agent and the others in the original group are set to 0.

## Strategy update

Entities stochastically update their strategies in response to resource scarcity. Specifically, the probability that an update occurs is given by  $\max\left(1 - \frac{r_i}{\theta}, 0\right) \cdot p_{SU}$ , where  $p_{SU}$  is a parameter controlling the frequency of strategy update events. An entity  $i$  that updates its strategy stochastically selects another entity  $j$  as its role model, with the probability given by

$$Q(j|i) = \frac{R_j}{\sum_{\substack{k \neq i \\ R_k > \theta}} R_k} \quad (3.8)$$

where  $\theta$  denotes the relevant threshold, i.e.,  $\theta_R$  at the group level and  $\theta_F$  at the agent level. The adopted strategy is then subject to mutation with probability  $\mu$ , resulting in a stochastic switch between  $C$  and  $D$ . After the update, all edges of the updated entity are reset to the baseline weight  $w_0$ .

## Evaluation

To examine how environmental variability and agent mobility influence the evolution of cooperation, we conduct simulations across a range of parameter settings, as summarized in Table 3.1. For each setting, 100 independent runs of 10000 generations are carried out. As the principal

performance indicators, we calculate the cooperation rates  $\phi_R^C$  and  $\phi_F^C$ , defined as the average proportions of groups and agents, respectively, employing strategy  $C$  during the last 5000 generations and averaged over all runs.

Table 3.1: Model parameters used in the simulations.

Parameter	Description	Value options
$n_R$	Number of regional groups	$10 \times 2^{\{0,1,2,3\}}$
$n_F$	Number of agents	$100 \times 2^{\{0,1,2,3,4,5,6\}}$
$\phi_C^0$	Initial frequency of cooperators	$\{0, 0.5, 1\}$
$w_0$	Initial edge weight	$\{0, 0.1, \dots, 1.0\}$
$p_{EV}$	Probability factor for environmental variability	$\{0, 0.1, \dots, 1.0\}$
$\theta_R$	Resource threshold at group level	0.5
$b$	PGG multiplier	$\{1.0, 1.1, \dots, 2.0\}$
$\Delta w$	Update rate of edge weights	$\{0, 0.1, \dots, 1.0\}$
$p_M$	Probability factor for migration events	$\{0, 0.1, \dots, 1.0\}$
$p_{SoR}$	Probability of migrating toward SoR	$\{0, 0.1, \dots, 1.0\}$
$p_{SU}$	Probability factor for strategy update events	0.1
$\mu$	Mutation probability in strategy update	$\{0, 0.01, 0.05, 0.1\}$

## 3.2 Results

### Influence of environmental variability and agent mobility

We conducted computational experiments to investigate how the environmental variability ( $p_{EV}$ ) and the agent mobility ( $p_M$ ) affect the cooperation rates at both the group ( $\phi_C^R$ ) and agent levels ( $\phi_C^F$ ).

Both  $\phi_C^R$  and  $\phi_C^F$  increase with  $p_{EV}$ , though with different patterns. At the group level (Figure 3.2a),  $\phi_C^R$  values are around 0.5 at  $p_{EV} = 0$ , increase sharply to approximately 0.7 by  $p_{EV} = 0.1$ , and then increase gradually to approximately 0.8 for  $p_{EV} > 0.1$ . This pattern does not depend on  $p_M$ . At the agent level (Figure 3.2b),  $\phi_C^F$  values are below 0.1 at  $p_{EV} = 0$  except at  $p_M = 0$ ; however, they increase steeply by  $p_{EV} = 0.1$  and plateau at levels determined by  $p_M$  for  $p_{EV} > 0.1$ .

While  $p_M$  does not affect  $\phi_C^R$  (Figure 3.2c),  $p_M$  significantly influences  $\phi_C^F$  (Figure 3.2d). When  $p_{EV} > 0$ ,  $\phi_C^F$  is approximately 0.6 at  $p_M = 0$ , increases to 0.8–0.9 at  $p_M = 0.1$ , and then decreases linearly for  $p_M > 0.1$ . In contrast, when  $p_{EV} = 0$ ,  $\phi_C^F$  starts at approximately 0.45 at  $p_M = 0$  and declines rapidly as  $p_M$  increases.

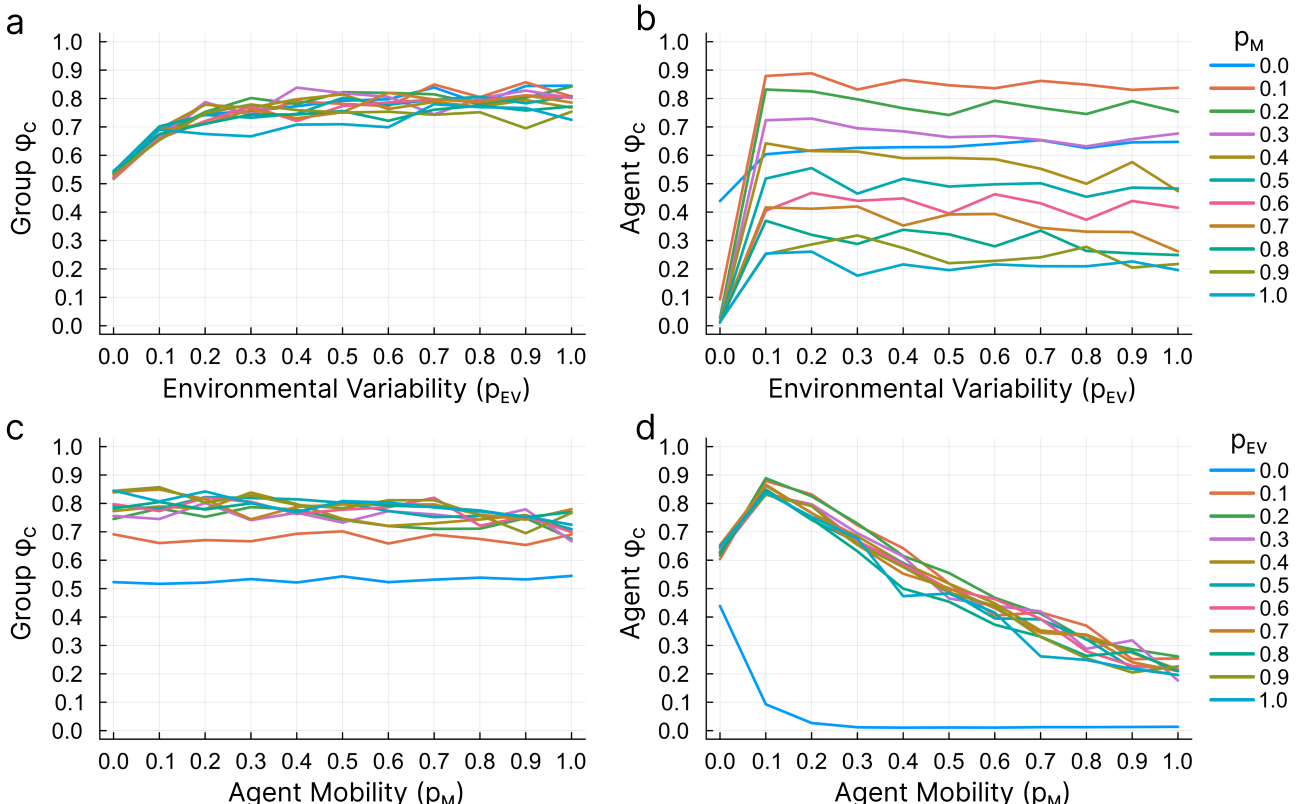


Figure 3.2: Average cooperation rates as functions of  $p_{EV}$  and  $p_M$ . (a)  $\phi_C^R$  vs.  $p_{EV}$  for different  $p_M$  values. (b)  $\phi_C^F$  vs.  $p_{EV}$  for different  $p_M$  values. (c)  $\phi_C^R$  vs.  $p_M$  for different  $p_{EV}$  values. (d)  $\phi_C^F$  vs.  $p_M$  for different  $p_{EV}$  values. Each data point represents the mean across 100 independent trials, where each trial is averaged over the final 5000 generations. Other parameters:  $n_R = 10$ ,  $n_F = 100$ ,  $\phi_C^0 = 0.5$ ,  $w_0 = 0.3$ ,  $\theta_R = 0.5$ ,  $b = 1.9$ ,  $\Delta w = 0.1$ ,  $p_{SoR} = 0.1$ ,  $\mu = 0.01$ .

Figure 3.3 shows standard deviations corresponding to Figure 3.2. Although the mean values exhibit clear patterns (Figure 3.2), the high inter-trial variability arises because  $\phi_C^R$  and  $\phi_C^F$  do not stabilize over time within each individual trial, with different trials converging toward either 0 or 1.

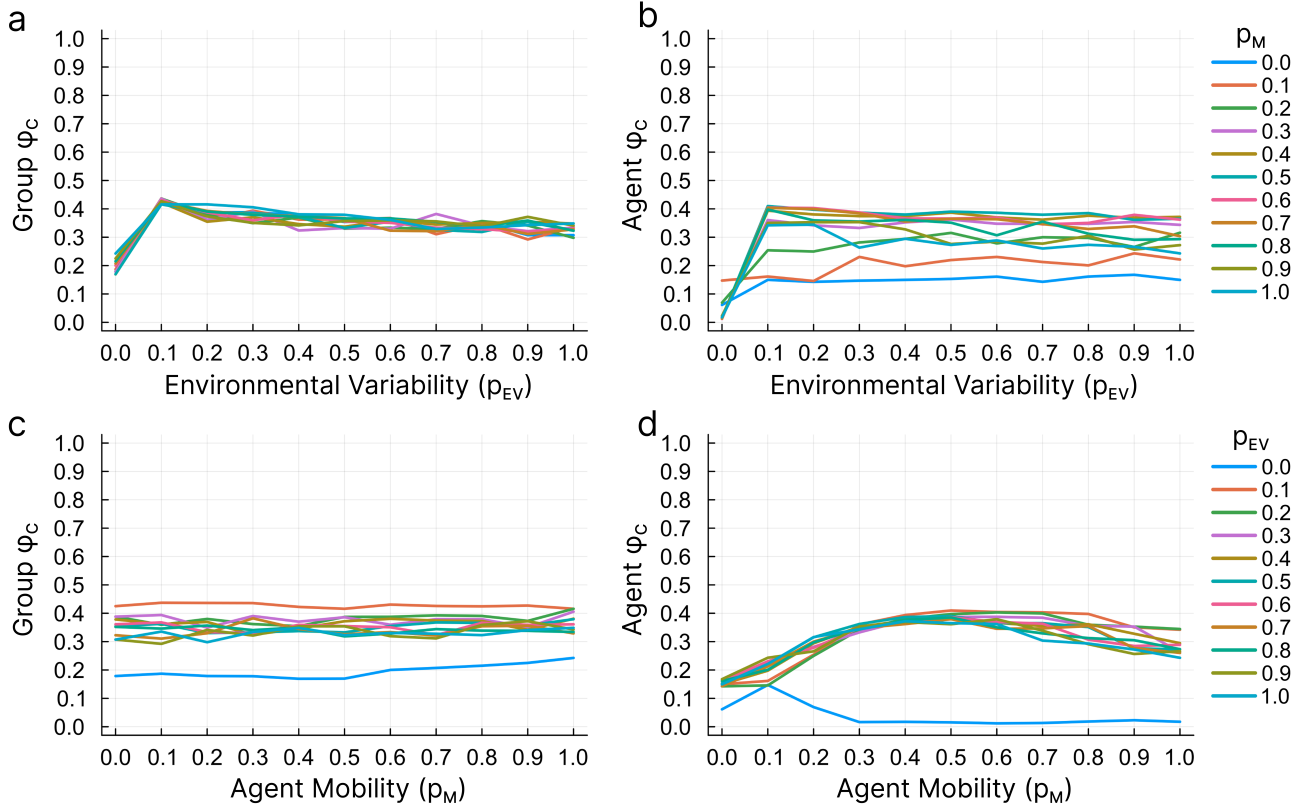


Figure 3.3: Standard deviations corresponding to Figure 3.2.

To examine the direction of influence between the group-level and agent-level processes, we conducted ablation experiments by selectively disabling specific model components. The results show that disabling agent-level games, migration, and strategy updates does not significantly affect  $\phi_C^R$  values (compare Figure 3.2a,c to Figure 3.4a,c), whereas disabling group-level games and strategy updates markedly suppresses  $\phi_C^F$  values (compare Figure 3.2b,d to Figure 3.4b,d). This asymmetry indicates that group-level processes contribute to agent-level cooperation, while the reverse influence is minimal.

The evolution of group-level cooperation by environmental variability can be explained by temporal resource distribution patterns (Figure 3.5). When  $p_{EV} = 0$ , the resource-rich region remains fixed at group 1, creating persistent spatial inequality where groups near SoR remain resource-rich and maintain stable strategies, while distant groups experience resource scarcity and undergo frequent strategy updates (Figure 3.5a). This spatial segregation prevents the formation of stable cooperative networks across the entire groups. In contrast, when  $p_{EV} > 0$ , the location of the resource-rich region shifts over time, ensuring that all regions experience both resource-rich and resource-poor periods. This temporal equity increases the long-term value of

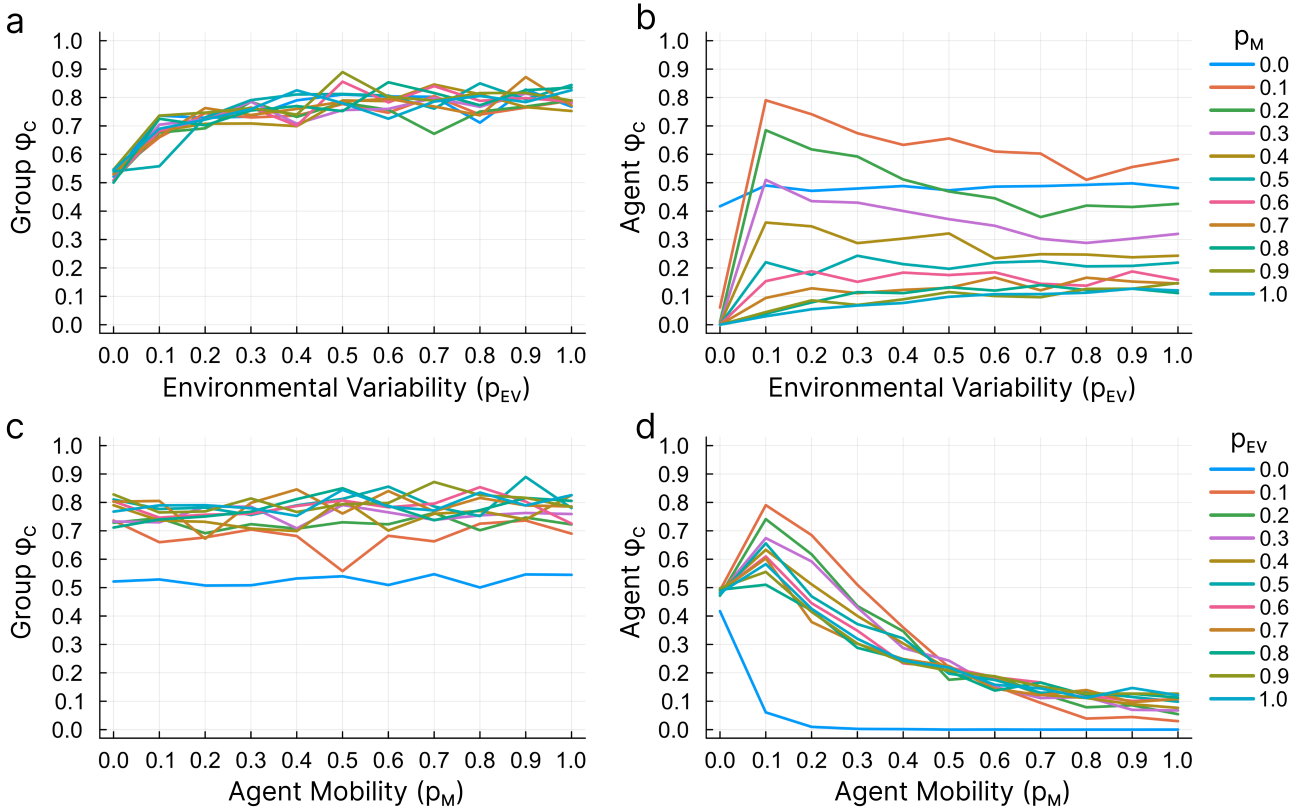


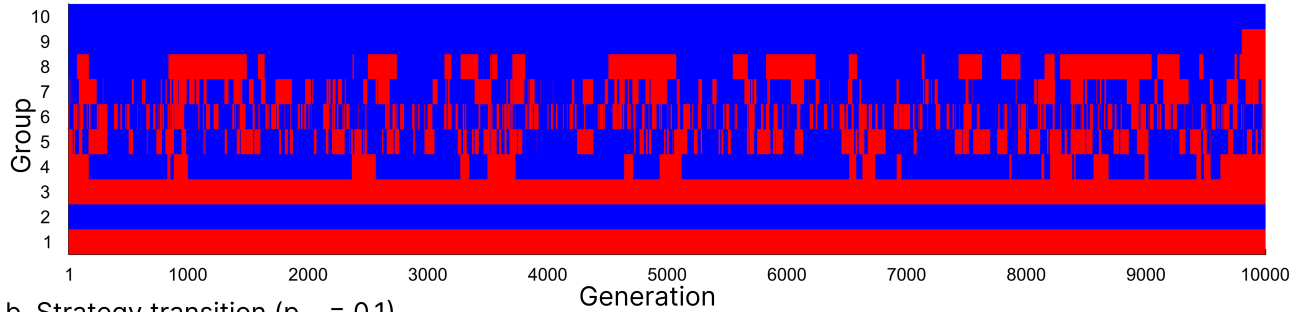
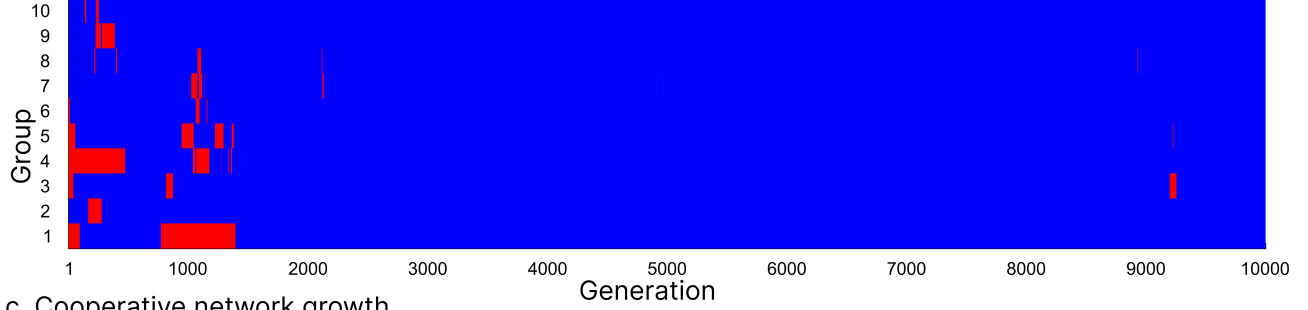
Figure 3.4: Ablation experiments corresponding to Figure 3.2. (a) and (c) show  $\phi_C^R$  when agent level games, migration, and strategy updates are disabled. (b) and (d) show  $\phi_C^F$  when group level games and strategy updates are disabled. Comparison with Figure 3.2 reveals that  $\phi_C^R$  maintains similar patterns regardless of agent level processes, whereas  $\phi_C^F$  is substantially reduced without group level processes. Other conditions are identical to Figure 3.2.

maintaining cooperative relationships through inter-regional games. As shown in Figure 3.5c, cooperative networks gradually form and stabilize throughout the population. Groups adopting  $C$  strategies build strong reciprocal relationships, while defecting regions become isolated. These cooperative networks provide resilience against both resource fluctuations and occasional mutations.

**ToDo:** The evolution of agent-level cooperation by environmental variability can be explained by ...

## Influence of population-related parameters

Figure 3.6 shows the effects of population size parameters  $n_R$  and  $n_F$  on cooperation rates under different environmental and mobility conditions.

a. Strategy transition ( $p_{EV} = 0$ )b. Strategy transition ( $p_{EV} = 0.1$ )

c. Cooperative network growth

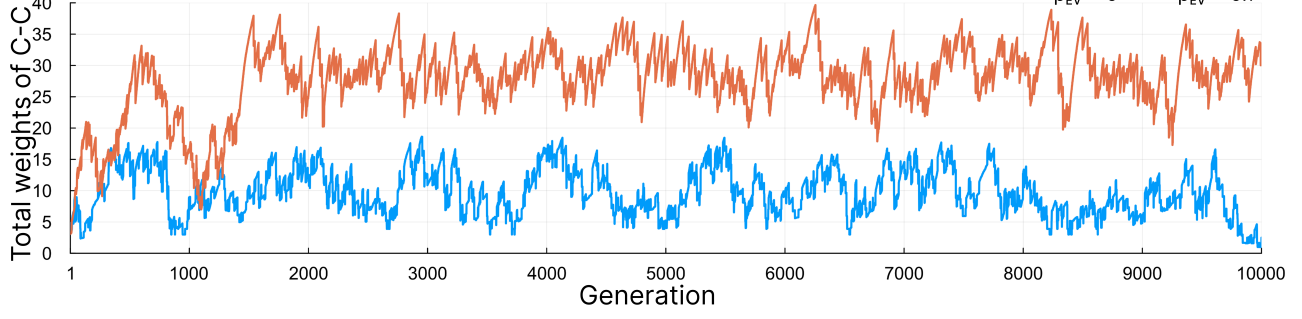
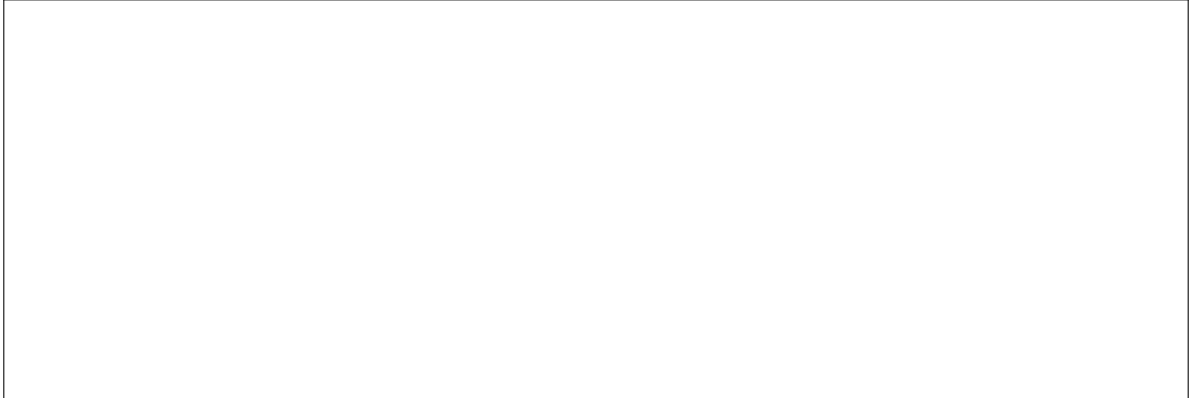


Figure 3.5: Temporal evolution of group-level cooperation. The horizontal axis represents generation, and the vertical axis represents group index. Blue indicates  $C$  and red indicates  $D$ . (a) shows the case where  $p_{EV} = 0$  with the resource-rich region fixed at group 1. (b) shows the case where  $p_{EV} = 0.1$  with a shifting resource-rich region. Occasional mutations introduce  $D$ , but they quickly revert to  $C$ . (c) shows the the transition of the sum of weights between  $C$  and  $C$ . Other conditions are identical to Figure 3.2.

Figure 3.6: Placeholder figure for population size effects ( $n_R$ ,  $n_F$ ) under varying  $p_{EV}$  and  $p_M$ .

When  $p_{EV} = 0.0$  and  $p_M = 0.0$ , both  $n_R$  and  $n_F$  have negligible effects on  $\phi_C^R$  and  $\phi_C^F$

(Figure 3.6a,b). When  $p_{EV} = 0.0$  and  $p_M = 0.1$ ,  $\phi_C^R$  remains unaffected by population sizes (Figure 3.6c), whereas  $\phi_C^F$  increases with both  $n_R$  and  $n_F$  (Figure 3.6d).

Under dynamic environmental conditions with  $p_{EV} = 0.5$  and  $p_M = 0.0$ ,  $\phi_C^R$  decreases slightly with increasing  $n_R$  but remains largely unaffected by  $n_F$  (Figure 3.6e). At the agent level,  $\phi_C^F$  decreases slightly with increasing  $n_R$  but increases slightly with increasing  $n_F$  (Figure 3.6f). These patterns remain essentially unchanged when  $p_M$  increases to 0.1 (Figure 3.6g,h).

The initial cooperation rate  $\phi_C^0$  influences the evolutionary outcomes (Figure 3.7).



Figure 3.7: Placeholder figure for effects of initial cooperation rate  $\phi_C^0$ .

When  $\phi_C^0 = 0$ , cooperation rates are lower overall compared to  $\phi_C^0 = 0.5$  (Figure 3.2), but the qualitative patterns remain unchanged. In contrast, when  $\phi_C^0 = 1$ , the patterns change dramatically. Both  $\phi_C^R$  and  $\phi_C^F$  approach 1.0 when  $p_{EV} = 0$  and decline as  $p_{EV}$  increases. Similarly, both cooperation rates approach 1.0 when  $p_M$  ranges from 0 to 0.1 and decline as  $p_M$  increases beyond this range.

## Influence of network parameters

The initial network weight  $w_0$  influences cooperation evolution at both levels, with smaller values promoting higher cooperation rates (Figure 3.8).

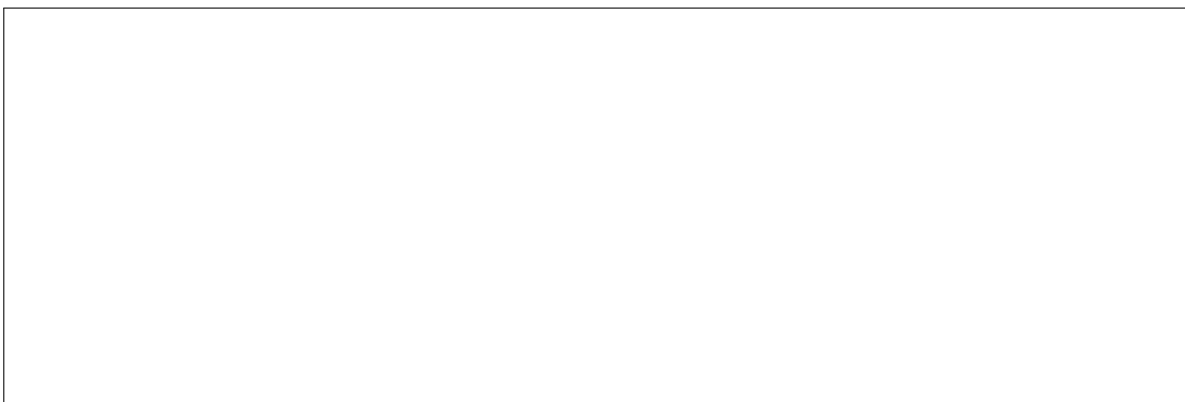


Figure 3.8: Placeholder figure for effects of initial network weight  $w_0$ .

This occurs because  $w_0$  determines the interaction strength with newcomers introduced through strategy updates or migration. When  $w_0$  is small, newcomers have weak initial relationships with existing members, limiting their immediate impact on the system. If a newcomer adopts defection, the low  $w_0$  prevents strong interactions that could disrupt established cooperative networks. In contrast, when  $w_0$  is large, defecting newcomers immediately engage in strong interactions with cooperative members, potentially destabilizing the cooperative network and reducing overall cooperation rates.

The relation weight update rate  $\Delta w$  positively affects cooperation, with higher values promoting cooperation at both levels (Figure 3.9).

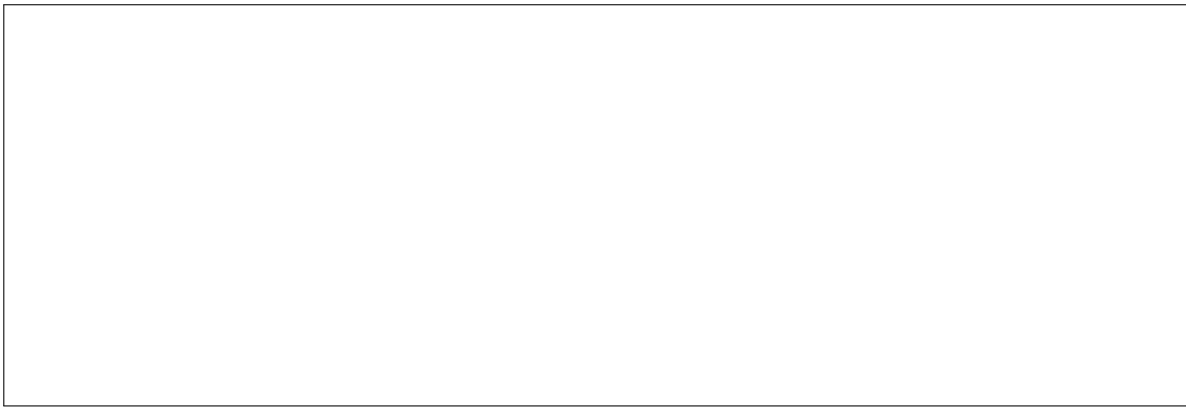


Figure 3.9: Placeholder figure for effects of relation weight update rate  $\Delta w$ .

Higher  $\Delta w$  values enable relation weights between  $C$  pairs to rapidly increase and those between  $D$  pairs to quickly decline, thereby accelerating the differentiation between  $C$  and  $D$  relationships. This rapid differentiation amplifies the benefits of cooperation and the costs of defection, strengthening selection pressures that favor cooperative strategies. However, cooperation rates saturate at approximately  $\Delta w = 0.3$  as they approach their maximum possible values, beyond which further increases in  $\Delta w$  have minimal additional effects.

## Influence of other parameters

We examined the effects of several additional parameters: the SoR orientation ( $p_{SoR}$ ), the PGG multiplier ( $b$ ), and the mutation rate ( $\mu$ ). The parameter  $p_{SoR}$  has no significant effect on cooperation rates. Higher values of  $b$  promote cooperation at both levels, as expected from standard public goods game theory. Higher  $\mu$  values blur the patterns observed in mean cooperation rates while reducing inter-trial variability, but do not alter the qualitative patterns. Since these results are either trivial or follow directly from model assumptions, detailed results are provided in the Supplementary Material.

# Chapter 4

## The 2-dimensional model with migration

**NOTE:** This chapter is based on the following preprint and will be edited for the dissertation format. Currently, only the Model and Results sections from the paper have been inserted as placeholders.

Inaba, M., Akiyama, E., 2025. Evolution of cooperation among migrating resource-oriented agents under environmental variability. arXiv [physics.soc-ph].[70]

Although previous studies have investigated cooperation under environmental variability and cooperation with mobility, no studies have integrated both the factors. Motivated by our interest in environmental variability and human behavioral evolution during the MSA in Africa, this study focuses on how environmental variability and agent mobility jointly affect the evolution of cooperation.

### 4.1 Model

In this study, we developed a multiagent simulation model to examine how agent mobility and environmental variability jointly influence the evolution of cooperation in spatially structured populations. Due to the limited availability of archaeological data on spatial resource distributions and hominin behavioral patterns during the MSA, we adopted an abstracted approach that prioritizes the identification of fundamental mechanisms over reproducing specific historical scenarios. This model incorporates four key processes, i.e., (i) environmental variability on a two-dimensional (2D) lattice, (ii) pairwise game interactions, (iii) conditional agent migration driven by resource availability, and (iv) strategy updating. These processes are described in the following subsections.

## Environmental variability

The spatial structure is represented by a 2D lattice with periodic boundary conditions. Here,  $N$  agents are distributed randomly across the cells, and each cell contains at most one agent. Each cell maintains a resource level that varies both spatially and temporally. We define a Source of Resources (SoR) as a focal point that generates spatial resource gradients in the environment, and these SoRs serve as simplified representations of the natural foraging areas commonly found near rivers, lakes, and coastlines. Each SoR creates a gradient where resource availability typically decreases with increasing distance from the SoR. In addition, multiple SoRs may coexist, thereby forming overlapping zones of resource abundance.

In this model, each agent accumulates resources (represented by the agent's fitness value) through interactions, and local prosperity is defined by a resource threshold  $\theta_{x,y}$  for each cell  $(x, y)$ , where  $0 \leq \theta_{x,y} \leq 1$ . Agents with fitness values that are less than the threshold  $\theta_{x,y}$  are more likely to migrate and update their strategies, and agents with fitness values greater than the threshold remain unchanged. Therefore, locations with lower thresholds impose less pressure for behavioral change, indicating that these locations are prosperous and rich in resources. Here, the threshold  $\theta_{x,y}$  is determined by the cumulative influence of all SoRs and is calculated as follows:

$$\theta_{x,y} = \frac{D_{x,y} - D_{\min}}{D_{\max} - D_{\min}}, \quad D_{x,y} = \sum_{i=1}^n d_{x,y}^{(i)} \quad (4.1)$$

where  $d_{x,y}^{(i)}$  denotes the Euclidean distance from cell  $(x, y)$  to the  $i$ -th SoR, calculated under periodic boundary conditions, and  $D_{\min}$  and  $D_{\max}$  denote the minimum and maximum values of  $D_{x,y}$  across the entire grid, respectively.

We examine two spatial configurations, which we refer to as 1-SoR and 2-SoR. In the 1-SoR configuration (a  $200 \times 200$  grid), a single SoR generates a concentric resource gradient, capturing the essential geographical pattern of an oasis-like environment (Figure 4.1a). In the 2-SoR configuration (a  $400 \times 200$  grid), two SoRs generate a corridor of resource gradient, capturing the essential geographical pattern of riverine or coastal environments where resources are distributed along a line (Figure 4.1b).

Environmental variability is modeled through the stochastic movement of SoRs, reflecting the unpredictable nature of the landscape dynamics observed during the MSA in Africa. Each SoR moves to a randomly selected adjacent cell within the Moore neighborhood with a probability  $p_{EV}$  ( $0 \leq p_{EV} \leq 1$ ) at each time step, and the direction is selected uniformly at random from the eight neighboring cells. In this process, the parameter  $p_{EV}$  governs the intensity of the environmental variability, where  $p_{EV} = 0$  corresponds to a static environment, and higher  $p_{EV}$  values represent more intense environmental variability.

Throughout this study, the neighborhood is defined as the Moore neighborhood (i.e., eight neighboring cells). This choice better approximates the continuous spatial movement of SoRs and mobile agents than the von Neumann neighborhood (i.e., four orthogonal cells), where

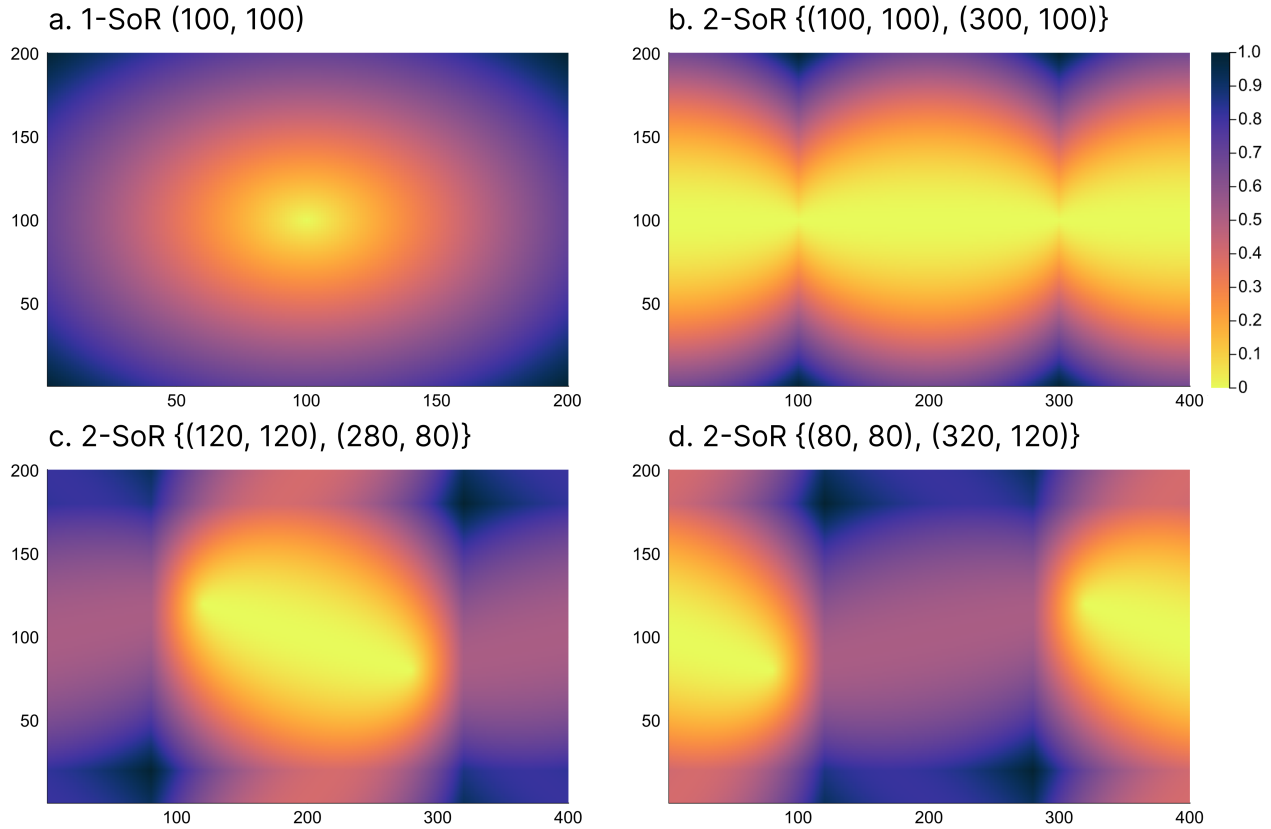


Figure 4.1: Spatially heterogeneous prosperity patterns generated by SoR(s). The colors indicate the resource threshold  $\theta_{x,y}$ . (a) A single SoR located at  $(100, 100)$  on a  $200 \times 200$  grid generates a concentric resource gradient. (b) Two SoRs located at  $(100, 100)$  and  $(300, 100)$  on a  $400 \times 200$  grid generate a band-shaped resource gradient. (c) and (d) Examples of SoR shifts over time.

movement is restricted to only cardinal directions. In addition, for distance calculations, particularly when determining resource gradients from SoRs, the Euclidean distance is employed to produce smooth, circular gradients that better represent natural resource distributions than other metrics, e.g., the Manhattan or Chebyshev distances.

## Game

Games represent cooperative or competitive interactions between agents that involve the gain or loss of resources. Each agent holds a strategy, either cooperation ( $C$ ) or defection ( $D$ ), which determines its behavior in interactions. In every time step, each agent plays pairwise games with all its neighbors and accumulates a payoff  $\pi_j$ , which is then converted into fitness  $\omega_j$  ( $j \in [1, \dots, N]$ ,  $0 < \omega_j < 1$ ), representing the agent's resource level.

The payoff matrix of the game is defined as follows:

$$\begin{array}{c|cc} & C & D \\ \hline C & R & S \\ D & T & P \end{array} \quad (4.2)$$

where  $R = 1$ ,  $0 < T < 2$ ,  $-1 < S < 1$ , and  $P = 0$ . To ensure the robustness of the results across a range of social dilemma contexts, we consider various game structures, including the Prisoner's Dilemma ( $T > R > P > S$ ), Stag Hunt ( $R > T > P > S$ ), and Snowdrift ( $T > R > S > P$ ) games.

The accumulated payoff  $\pi_j$  is transformed into the fitness  $\omega_j$  using a sigmoid function as follows:

$$\omega_j = \frac{1}{1 + \exp(-k(\pi_j - \pi_0))} \quad (4.3)$$

where  $k$  determines the steepness of the sigmoid curve, and  $\pi_0$  sets the baseline payoff at which  $\omega_j = 0.5$ . Here, we set  $k = 1$  for moderate sensitivity and set  $\pi_0 = 4.0$  to center the sigmoid around common payoff values found in mixed-strategy populations. Given that each agent can accumulate payoffs from up to eight of its neighbors, the theoretical payoff range is  $8S$  to  $8R$  and  $8P$  to  $8T$  for cooperators and defectors, respectively. With our parameter constraints, this yields a payoff range of  $-8 < \pi_j < 16$ .

## Migration

At each time step, agents migrate if their fitness  $\omega_j$  is less than the resource threshold  $\theta_{x,y}$  at their current location. Any agent that meets this condition migrates with probability  $p_M$  and remains at the location with the complementary probability  $1 - p_M$ . The migration direction follows a resource-oriented bias, where an agent moves toward a neighboring cell with the lowest  $\theta_{x,y}$  value with probability  $p_{SoR}$  (SoR orientation) and moves randomly within the neighborhood with the complementary probability  $1 - p_{SoR}$ . Cells occupied by other agents are excluded from the candidate destinations. The agents migrate asynchronously in a randomized order to avoid movement conflicts.

## Strategy update

At each time step, agents update their strategies synchronously if their fitness  $\omega_j$  is less than the resource threshold  $\theta_{x,y}$ . Any agent that meets this condition adopts the strategy of the most successful neighbor (i.e., the neighbor with the highest fitness). This process is subject to mutation, where the adopted strategy is replaced by the opposite strategy (e.g., from  $C$  to  $D$  or vice versa) with probability  $\mu$ .

## Evaluation

To investigate the effects of environmental variability and agent mobility on the evolution of cooperation, simulations are performed under a range of parameter configurations, as shown in Table 4.1.

Each configuration is evaluated through 100 independent trials of 10000 generations each. As the primary outcome measure, we compute the cooperation rate  $\phi_C$ , which is defined as the average proportion of agents employing the  $C$  strategy during the final 5000 generations averaged over all trials.

Table 4.1: Model parameters used in the simulations.

Parameter	Description	Value options
$W \times H$	Grid dimensions	$200 \times 200, 400 \times 200$
$N$	Total number of agents	$500 \times 2^{\{0,1,2,3,4,5\}}$
$\phi_C^0$	Initial frequency of cooperators	0, 0.5, 1
$n_{SoR}$	Total number of SoRs	1, 2
$p_{EV}$	Probability of SoR shift	0 to 1 (step: 0.1)
$R$	Payoff for mutual cooperation	1
$T$	Payoff for defection against cooperator	0 to 2 (step: 0.1)
$P$	Payoff for mutual defection	0
$S$	Payoff for cooperation against defector	-1 to 1 (step: 0.1)
$p_M$	Probability of migration	0 to 1 (step: 0.1)
$p_{SoR}$	Probability of resource-oriented migration	0 to 1 (step: 0.1)
$\mu$	Probability of mutation	0, 0.01

## 4.2 Results

### Influence of environmental variability and agent mobility

Figure 4.2 shows the combined effects of environmental variability ( $p_{EV}$ ) and agent mobility ( $p_M$ ) on the cooperation rate  $\phi_C$ . As can be seen, in stable environments ( $p_{EV} = 0$ ) or with low agent mobility ( $p_M \lesssim 0.2$ ), cooperation fails to evolve. In contrast, with sufficient agent mobility ( $p_M \gtrsim 0.2$ ), even modest environmental variability ( $p_{EV} = 0.1$ ) promotes cooperation; however, further variability ( $p_{EV} > 0.1$ ) does not enhance cooperation. In addition, agent mobility promotes cooperation with any level of environmental variability ( $p_{EV} > 0$ ).

Figure 4.3 shows the role of environmental variability in the evolution of cooperation. This representative simulation is presented to understand the temporal dynamics underlying the statistical patterns displayed in Figure 4.2. Whereas Figure 4.2 considers fixed variability levels throughout the simulation, here we apply a cyclic  $p_{EV}$  alternating between stable and variable conditions every 2000 generations over a total of 10000 generations. Under these cyclic conditions, cooperation initially increases to slightly less than 50% during the first stable phase

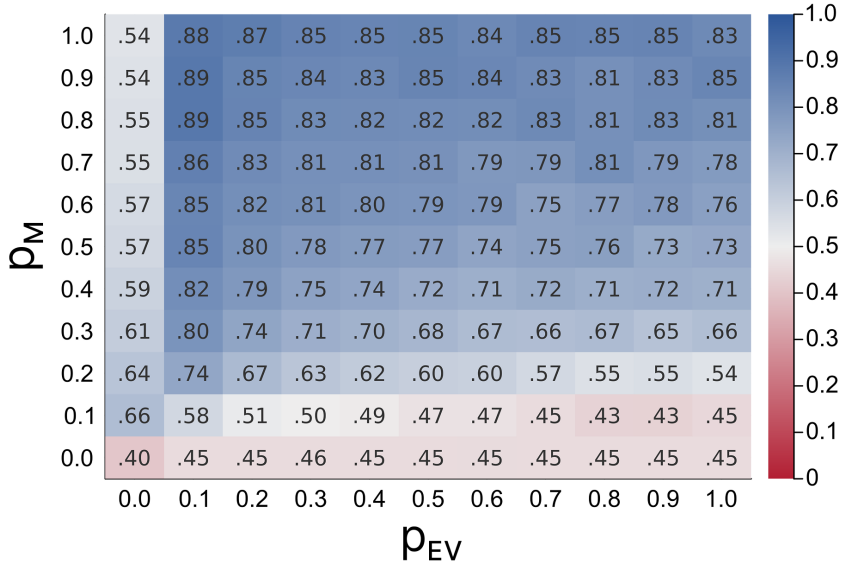


Figure 4.2: Influence of environmental variability ( $p_{EV}$ ) and agent mobility ( $p_M$ ) on the cooperation rate ( $\phi_C$ ). Each cell shows the mean over 100 independent runs. The results are shown for a representative parameter set ( $N = 1000$ ,  $\phi_C^0 = 0.0$ , 2-SoR,  $T = 1.2$ ,  $S = -0.2$ ,  $p_{SoR} = 0.1$ ,  $\mu = 0.01$ ). Qualitatively similar patterns are observed for other parameter configurations. The standard deviations across runs are  $< 0.15$  for all cells.

and then plateaus, as shown in Figure 4.3a. A pronounced increase is observed once the system enters the variable phase, which reinforces the conclusion that environmental variability plays a pivotal role in promoting cooperation.

The observed dynamics can be understood as a three-stage process: (i) the formation of a few large defector groups fixed in resource-rich areas, (ii) their collapse induced by environmental variability, and (iii) subsequent emergence of several small cooperator groups. Figures 4.3b–f show snapshots from the simulation presented in Figure 4.3a. A full video showing this process is provided in the Supplementary Material. In the first stable phase as shown in Figure 4.3b, the agents in prosperous areas have no need to cooperate or move, whereas those in less prosperous areas must cooperate or move to prosperous areas. At the boundaries between these two areas, fixed walls are formed by defectors who do not need to change their strategies or move further. During the next variable phase as shown in Figures 4.3c–e, agents located on boundaries are forced to cooperate or move due to the environmental changes, thereby leading to the collapse of the stable defector group as shown in the central area of Figure 4.3c. In place of the defector group, the agents form several small cooperator groups to survive even in severe environmental conditions (Figure 4.3d). Then, the same process occurs in the areas at both ends of the figure (Figures 4.3e and f).

In contrast, cooperation cannot evolve if the agent mobility is insufficient relative to the intensity of the environmental variability (refer to the lower area of Figure 4.2), which occurs because excessively rapid SoR movement prevents the formation of both defector structures and

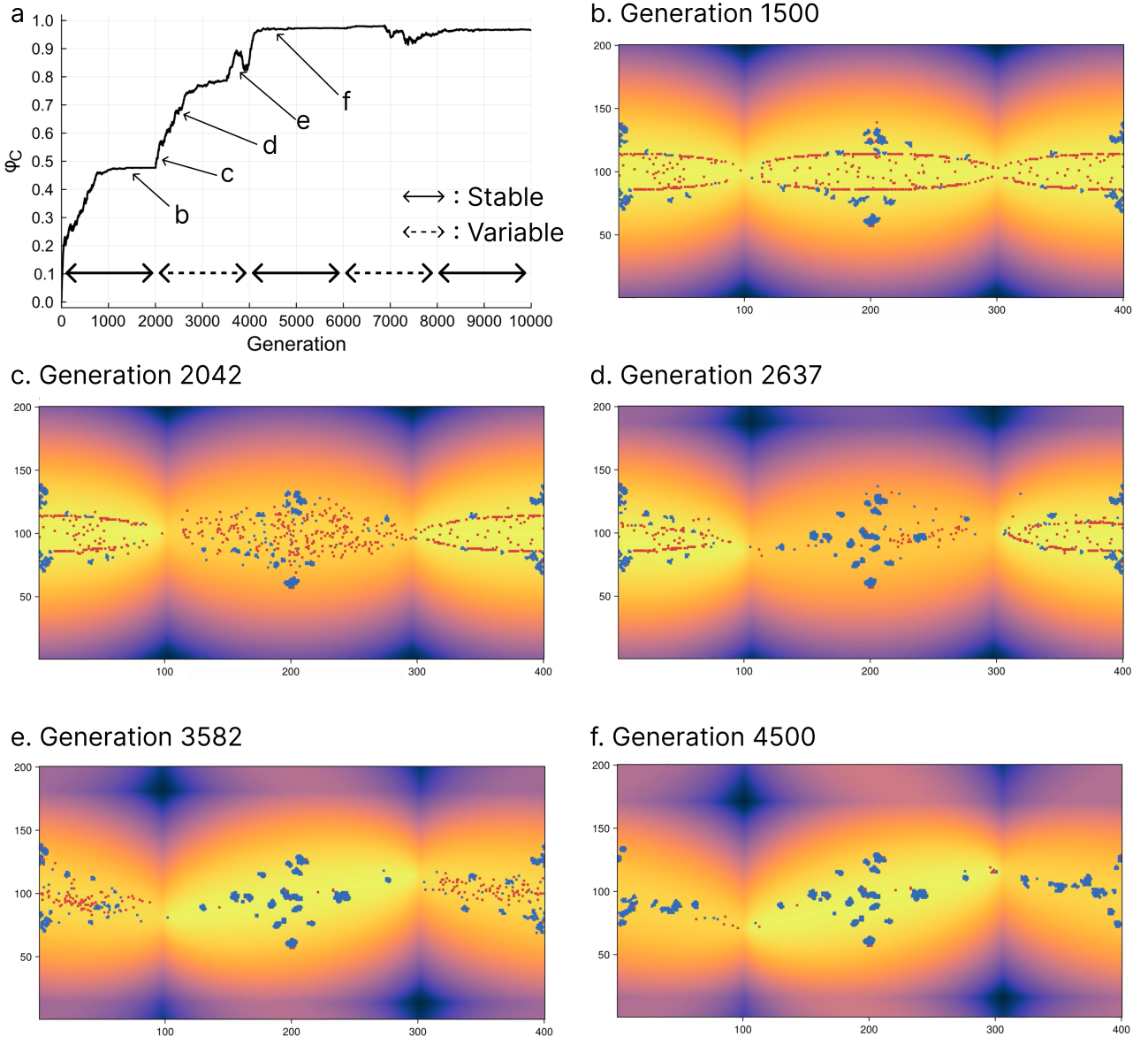


Figure 4.3: Temporal dynamics under cyclic environmental variability. Parameter settings:  $N = 1000$ ,  $\phi_C^0 = 0.0$ , 2-SoR,  $T = 1.2$ ,  $S = -0.2$ ,  $p_M = 1.0$ ,  $p_{SoR} = 0.1$ ,  $\mu = 0.01$ . The stable and variable phases correspond to  $p_{EV} = 0$  and  $p_{EV} = 0.1$ , respectively. The blue and red dots represent cooperators and defectors, respectively. The background colors indicate the resource threshold  $\theta_{x,y}$  as in Figure 4.1.

small cooperator groups, as shown in Figure 4.4. Thus, environmental variability and sufficient agent mobility promote cooperation by preventing fixed defector structures and encouraging the agents to form cooperator groups for survival.

## Influence of other parameters on cooperation rate

To gain further insights into the findings presented above and assess their robustness, we investigated the effects of additional parameters, including the population size ( $N$ ), the number of SoRs ( $n_{SoR}$ ), the initial frequency of cooperators ( $\phi_C^0$ ), the SoR orientation ( $p_{SoR}$ ), the payoff

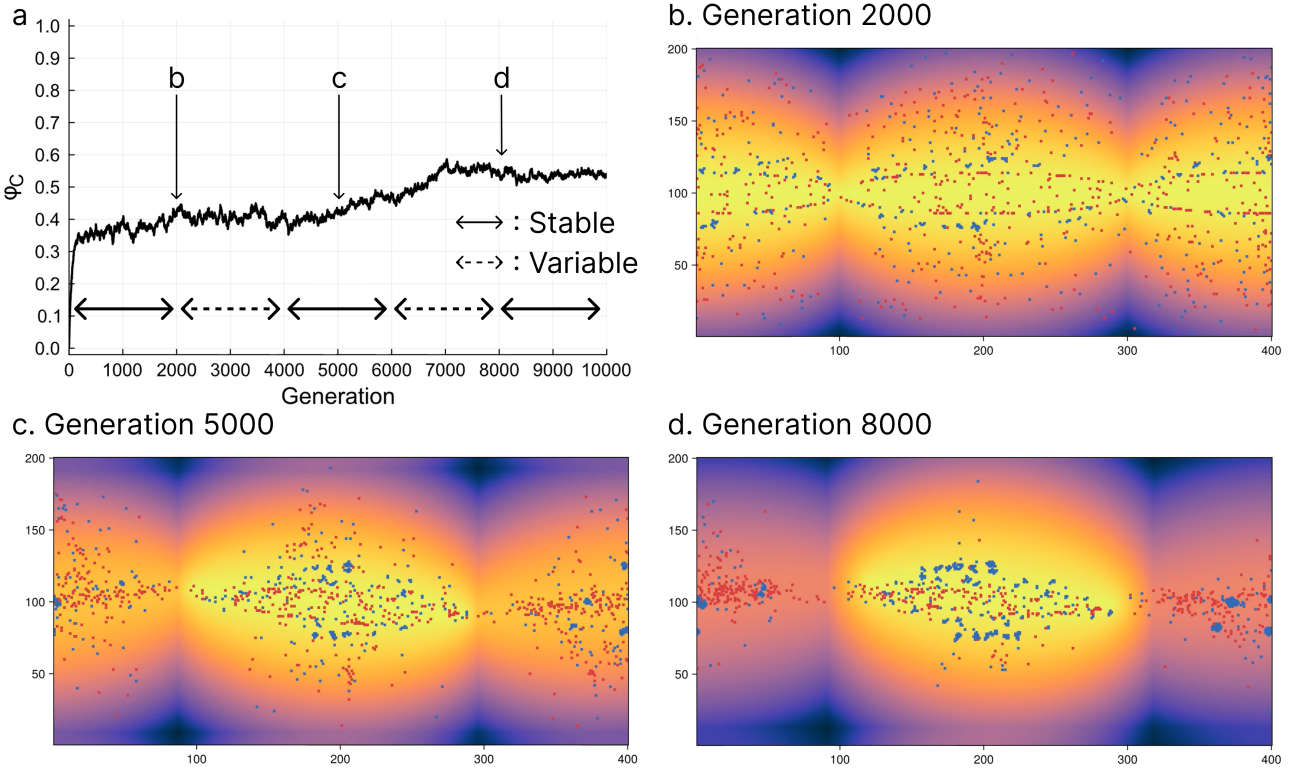


Figure 4.4: Temporal dynamics under cyclic environmental variability with low agent mobility. In contrast to Figure 4.3 ( $p_M = 1.0$ ), here, lower mobility ( $p_M = 0.1$ ) prevents the agents from keeping up with the environmental variability; thus, cooperation fails to stabilize. All other parameters and the interpretation of the visual elements are the same as in Figure 4.3.

parameters ( $T$ ,  $S$ ), and the mutation rate ( $\mu$ ).

### Population size

Larger population size promotes cooperation to some extent, as shown in Figure 4.5, because the cooperators can more easily find other cooperators when the population size is sufficiently large.

Another notable observation is that the cooperation rates for  $(p_{EV}, p_M) = (0.0, 0.1)$  (red dashed line) and  $(0.1, 0.1)$  (blue dashed line) exhibit a crossover at approximately  $N = 2000$ . For small populations ( $N < 2000$ ) with low agent mobility, cooperation evolves more readily without environmental variability. In stable environments ( $(p_{EV}, p_M) = (0.0, 0.1)$ ), both the defector and cooperator groups persist once established, although the formation of these groups is slow due to the low agent mobility. In contrast, environmental variability with low agent mobility ( $(p_{EV}, p_M) = (0.1, 0.1)$ ) creates perpetual fluidity that prevents the formation of both structures.

Larger populations alter this relationship. Larger populations increase the encounter rate among cooperators, which allows for the formation of cooperator groups even under environmental variability. In stable environments, the structures remain fixed, thereby limiting the impact of the higher encounter rate. In contrast, the higher encounter rate in fluid environ-

ments facilitates group formation. Thus, environmental variability becomes advantageous for cooperation above the critical population size.

A less prominent but similar crossover occurs at approximately  $N = 8000$  between  $(p_{EV}, p_M) = (0.0, 0.1)$  (red dashed line) and  $(p_{EV}, p_M) = (0.0, 1.0)$  (red solid line). This crossover reflects the spatial constraints of the defector groups in stable environments ( $p_{EV} = 0$ ). For  $N \lesssim 8000$ , high mobility ( $p_M = 1.0$ ) allows more agents to reach the resource-rich areas where cooperation is not required. In contrast, low mobility ( $p_M = 0.1$ ) keeps the agents in peripheral areas where cooperation is required for survival.

However, larger populations ( $N \gtrsim 8000$ ) exhibit three nested zones: central rich areas, where cooperation is not required; surrounding moderate areas, where the agents can survive through cooperation; and the most peripheral harsh areas, where agents cannot survive even with cooperation because the resource threshold exceeds what can be provided through cooperation. Under these conditions, high mobility allows the agents to escape from the harsh areas to the moderate cooperative areas, whereas low mobility traps the agents in the harsh areas. In addition, the central rich areas have already reached their physical capacity due to the large population; thus, further population increases have no effect in these areas. Consequently, the effect of mobility on the cooperation rate ( $\phi_C$ ) reverses as the population size increases.

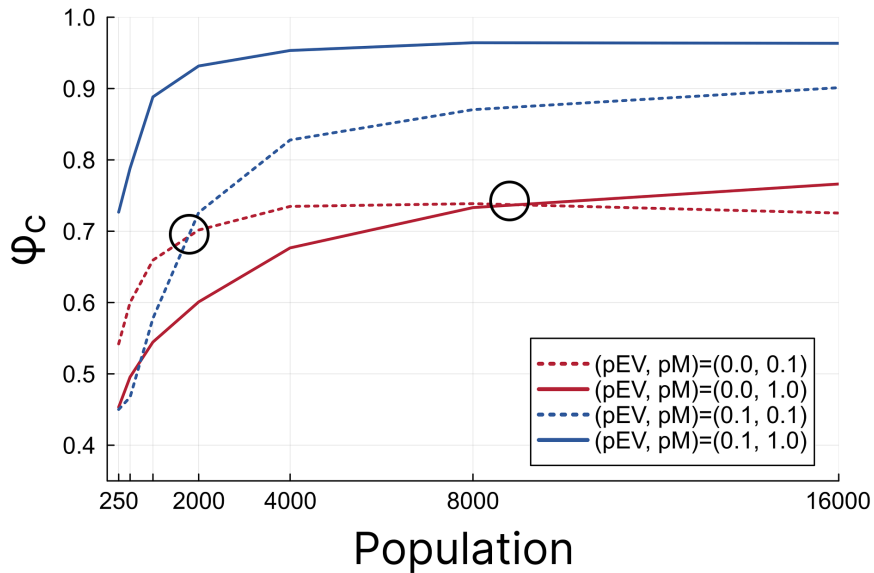


Figure 4.5: Influence of population size ( $N$ ) on cooperation rate ( $\phi_C$ ). Parameter settings:  $\phi_C^0 = 0.0$ , 2-SoR,  $T = 1.2$ ,  $S = -0.2$ ,  $p_{SoR} = 0.1$ ,  $\mu = 0.01$ . The results for  $N = 32000$  are omitted because they exhibited negligible differences from  $N = 16000$ .

### Number of SoRs and initial cooperator rate

Both the number of SoRs ( $n_{SoR}$ ) and the initial frequency of cooperators ( $\phi_C^0$ ) have a significant influence on the results. While the 2-SoR configuration forms large band-shaped defector

groups (Figure 4.3b), the 1-SoR configuration only forms a small, circular resource-rich area (Figure 4.6b). When a large defector group collapses and is replaced by small cooperator groups, as observed with the 2-SoR setting, the impact on the overall system is substantial. In contrast, under the 1-SoR setting, when a small defector group undergoes the same replacement, the effect is less conspicuous than the 2-SoR setting (Figure 4.6a). In terms of  $\phi_C^0$ , initiation with no cooperators ( $\phi_C^0 = 0$ ) in the 2-SoR configuration results in large defector groups, whereas intermediate or full cooperation ( $\phi_C^0 = 0.5$  or 1) maintains the large structure but with a higher cooperator frequency within it (Figure 4.7). Consequently, these conditions mask the significant effects of defector group collapse and cooperator group formation observed in Subsection 4.2.

We also confirmed that changing the distance metric from Euclidean to the Chebyshev or Manhattan distance alters the size and shape of the groups, thereby affecting the results. However, these effects are primarily attributed to differences in the group size rather than shape. Thus, comparisons among these distance metrics can be interpreted as theoretically equivalent to the comparison between the 1-SoR and 2-SoR settings. Essentially, the formation of large defector groups in stable environments is the critical prerequisite for the results described in Subsection 4.2.

## SoR orientation

SoR orientation ( $p_{SoR}$ ) noticeably influences the cooperation rate (Figure 4.8). Increasing  $p_{SoR}$  from 0 to 0.1 improves cooperation rates by approximately 20%–40% if  $p_{EV} > 0$ . However, further increases in  $p_{SoR}$  beyond 0.2 reduce the cooperation rate. This reduction occurs because excessive  $p_{SoR}$  increases the likelihood of agent collisions, which in turn hinders effective migration. These findings suggest that some randomness in the agent mobility is required to maintain a high level of cooperation.

## Payoff parameters and mutation rate

We also investigated the effects of varying the values of the payoff parameters ( $T, S$ ) across several game structures and the mutation rate  $\mu$  (including  $\mu = 0$  and  $\mu = 0.01$ ). While these variations did not yield qualitatively new insights, they confirmed the robustness of the observed patterns. For completeness, the corresponding results are provided in the Supplementary Material.

## Summary

In this study, we examined the joint effects of environmental variability and agent mobility on the evolution of cooperation to understand the causal dynamics of these factors in spatially structured populations. The model incorporates unpredictable environmental variability

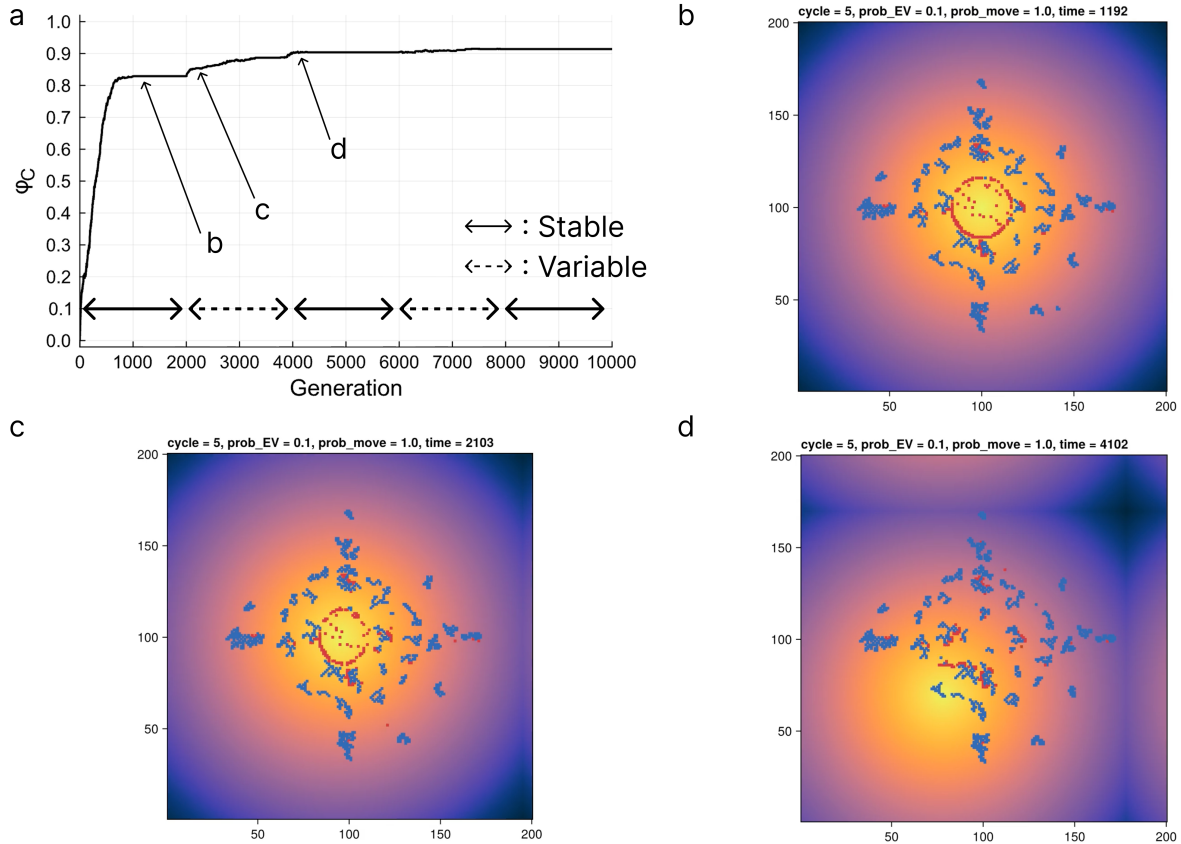


Figure 4.6: Temporal dynamics under cyclic environmental variability in the 1-SoR configuration. In contrast to Figure 4.3 (2-SoR configuration), the impact of the transition from defection to cooperation in the central resource-rich area is less pronounced in the 1-SoR configuration. All other parameters and the interpretation of the visual elements are the same as in Figure 4.3.

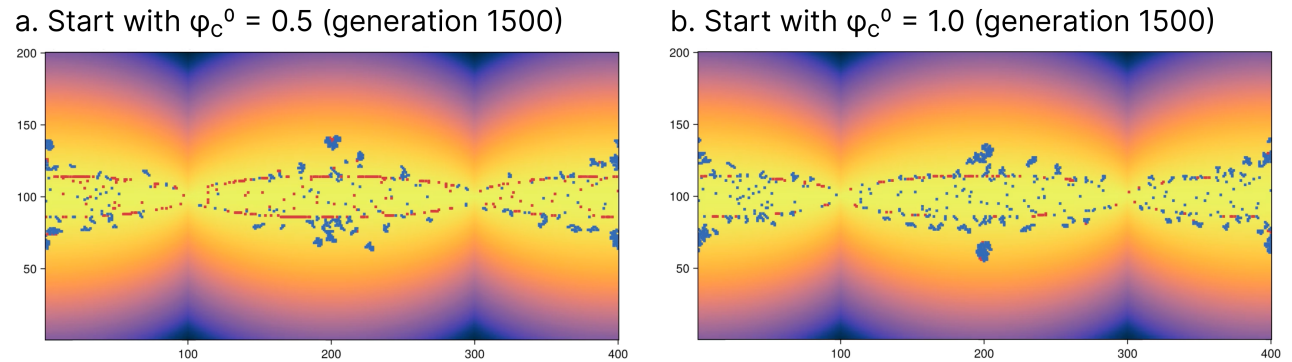


Figure 4.7: Central resource-rich areas under  $\phi_C^0 = 0.5$  or  $1.0$ . All parameters (except  $\phi_C^0$ ) and the interpretation of the visual elements are the same as in Figure 4.3.

by implementing SoRs that move randomly across a 2D space, generating dynamic spatial heterogeneity in resource availability. Agents accumulate resources through cooperative or competitive interactions, and the agents with lower resource levels are more likely to migrate to neighboring cells and update their strategies. With this model, we identified three key findings. First, with sufficient agent mobility, even modest environmental variability promotes cooperation; however, further variability does not enhance cooperation. Second, with any

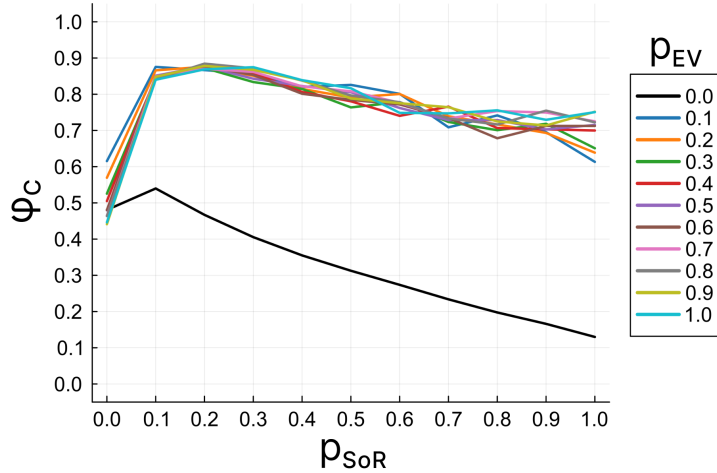


Figure 4.8: Influence of SoR orientation ( $p_{SoR}$ ) on the cooperation rate ( $\phi_C$ ). Parameter settings:  $N = 1000$ ,  $\phi_C^0 = 0.0$ , 2-SoR,  $p_M = 1.0$ ,  $T = 1.2$ ,  $S = -0.2$ ,  $\mu = 0.01$ .

level of environmental variability, agent mobility promotes cooperation. Third, these effects occur because environmental variability disrupts a few large stable defector groups that form in resource-rich areas, and agent mobility effectively enables the formation of numerous small cooperater groups at those sites.

# Chapter 5

## Conclusion

### 5.1 Summary of results

This dissertation investigated whether and how environmental variability (EV) promotes the evolution of cooperation through three distinct modeling approaches.

[TODO: Summarize key findings and mechanisms from Chapter 2]

[TODO: Summarize key findings and mechanisms from Chapter 3]

[TODO: Summarize key findings and mechanisms from Chapter 4]

[TODO: Summarize common and divergent findings across the three models, and the reasons].

[TODO: Summarize common and divergent mechanisms across the three models, and the reasons]

### 5.2 Implications and interpretation

The results of this dissertation have several implications for understanding the evolution of cooperation and human behavior.

First, our research extends the variability selection hypothesis (VSH) beyond individual cognitive adaptations. EV during the Middle Stone Age (MSA) has been primarily understood as a selective pressure on individual-level cognitive abilities, particularly brain expansion. Our research demonstrates that EV may have also directly influenced group-level social structures, extending the scope of VSH to encompass collective behavioral patterns. [TODO: Elaborate this paragraph]

Second, this dissertation identifies variability selection as a previously underexplored mechanism in cooperation theory. While numerous mechanisms for the evolution of cooperation have been proposed, variability selection has received limited attention as a potential driver of cooperation. Our findings demonstrate that variability selection can promote cooperation.

[TODO: Elaborate this paragraph]

Third, the theoretical insights from this research may inform future empirical work in evolutionary anthropology and archaeology. [TODO: Elaborate this paragraph]

### 5.3 Limitations and future directions

While this dissertation provides insights into the relationship between EV and cooperation, several limitations warrant acknowledgment and suggest directions for future research.

First, our theoretical findings lack direct empirical validation. Cooperative behaviors leave limited archaeological traces, making it challenging to test predictions against paleoenvironmental and archaeological data. Future empirical work integrating paleoclimatic records with archaeological evidence of social organization and resource sharing could test whether cooperation patterns correlate with periods of environmental variability. [TODO: Elaborate this paragraph.]

Second, the models employed in this research are too simple as representations of reality. The spatial structures, migration patterns, interaction mechanisms, and strategy updating rules could be modeled in numerous alternative ways. While the three modeling approaches serve as appropriate starting points, they are far from exhaustive, and substantial room remains for developing more diverse and realistic models. [TODO: Elaborate this paragraph.]

Third, the models are too complex for full analytical treatment. The three models examined in this dissertation incorporate sufficient detail to capture realistic dynamics but are consequently difficult to analyze mathematically. Future research could benefit from developing simpler, analytically tractable models that isolate key mechanisms identified in this work. [TODO: Elaborate this paragraph.]

# Appendix

## Data and code availability

All data, as well as the code required to run the simulations and generate the figures, are available at

- Chapter 2: <https://github.com/mas178/Inaba2024>
- Chapter 3: <https://github.com/mas178/Inaba2025-2Lvl>
- Chapter 4: <https://github.com/mas178/Inaba2025-2D>

## Supplementary material for Chapter 3

## Supplementary material for Chapter 4

# Bibliography

- [1] C. Darwin. On the origin of species. 1859.
- [2] C. Darwin. The descent of man, and selection in relation to sex. 1871.
- [3] W. Hamilton. The genetical evolution of social behaviour. I. *J. theor. biol.* 7.1 (1964), 1–16. DOI: [10.1016/0022-5193\(64\)90038-4](https://doi.org/10.1016/0022-5193(64)90038-4).
- [4] W. D. Hamilton. The genetical evolution of social behaviour. II. *J. theor. biol.* 7.1 (1964), 17–52. DOI: [10.1016/0022-5193\(64\)90039-6](https://doi.org/10.1016/0022-5193(64)90039-6).
- [5] M. A. Nowak, C. E. Tarnita, and E. O. Wilson. The evolution of eusociality. *Nature* 466.7310 (2010), 1057–1062. DOI: [10.1038/nature09205](https://doi.org/10.1038/nature09205).
- [6] P. Abbot, J. Abe, J. Alcock, S. Alizon, J. A. C. Alpedrinha, M. Andersson, et al. Inclusive fitness theory and eusociality. *Nature* 471.7339 (2011), E1–4, author reply E9–10. DOI: [10.1038/nature09831](https://doi.org/10.1038/nature09831).
- [7] M. van Veelen. The general version of hamilton’s rule. *Elife* (2025). DOI: [10.7554/elife.105065.1](https://doi.org/10.7554/elife.105065.1).
- [8] J. M. Smith and G. R. Price. The logic of animal conflict. *Nature* 246.5427 (1973), 15–18. DOI: [10.1038/246015a0](https://doi.org/10.1038/246015a0).
- [9] R. Axelrod and W. D. Hamilton. The evolution of cooperation. *Science* 211.4489 (1981), 1390–1396. DOI: [10.1126/science.7466396](https://doi.org/10.1126/science.7466396).
- [10] M. A. Nowak and K. Sigmund. Evolution of indirect reciprocity by image scoring. *Nature* 393.6685 (1998), 573–577. DOI: [10.1038/31225](https://doi.org/10.1038/31225).
- [11] M. A. Nowak and K. Sigmund. Evolution of indirect reciprocity. *Nature* 437.7063 (2005), 1291–1298. DOI: [10.1038/nature04131](https://doi.org/10.1038/nature04131).
- [12] H. Ohtsuki, C. Hauert, E. Lieberman, and M. A. Nowak. A simple rule for the evolution of cooperation on graphs and social networks. *Nature* 441.7092 (2006), 502–505. DOI: [10.1038/nature04605](https://doi.org/10.1038/nature04605).
- [13] A. Traulsen and M. A. Nowak. Evolution of cooperation by multilevel selection. *Proc. natl. acad. sci. u. s. a.* 103.29 (2006), 10952–10955. DOI: [10.1073/pnas.0602530103](https://doi.org/10.1073/pnas.0602530103).

- [14] M. A. Nowak. Five rules for the evolution of cooperation. *Science* 314.5805 (2006), 1560–1563.
- [15] S. A. West, A. S. Griffin, and A. Gardner. Evolutionary explanations for cooperation. *Curr. biol.* 17.16 (2007), R661–R672.
- [16] S. Mcbrearty and A. S. Brooks. The revolution that wasn't: a new interpretation of the origin of modern human behavior. *J. hum. evol.* 39.5 (2000), 453–563.
- [17] C. S. Henshilwood and C. W. Marean. The origin of modern human behavior: critique of the models and their test implications. *Curr. anthropol.* 44.5 (2003), 627–651.
- [18] F. d'Errico, A. Pitarch Martí, C. Shipton, E. Le Vraux, E. Ndiema, S. Goldstein, et al. Trajectories of cultural innovation from the middle to later stone age in eastern africa: personal ornaments, bone artifacts, and ocher from panga ya saidi, kenya. *J. hum. evol.* 141.102737 (2020), 102737.
- [19] J. Wilkins, B. J. Schoville, R. Pickering, L. Gliganic, B. Collins, K. S. Brown, et al. Innovative homo sapiens behaviours 105,000 years ago in a wetter kalahari. *Nature* 592.7853 (2021), 248–252.
- [20] A. Bergström, C. Stringer, M. Hajdinjak, E. M. L. Scerri, and P. Skoglund. Origins of modern human ancestry. *Nature* 590 (2021), 229–237.
- [21] R. Potts. Evolution and climate variability. *Science* 273.5277 (1996), 922–923.
- [22] R. Potts. Environmental hypotheses of hominin evolution. *Am. j. phys. anthropol.* Suppl 27 (1998), 93–136.
- [23] J. T. Faith, A. Du, A. K. Behrensmeyer, B. Davies, D. B. Patterson, J. Rowan, et al. Rethinking the ecological drivers of hominin evolution. *Trends ecol. evol.* 36.9 (2021), 797–807.
- [24] C. Schuck-Paim, W. J. Alonso, and E. B. Ottoni. Cognition in an ever-changing world: climatic variability is associated with brain size in neotropical parrots. *Brain behav. evol.* 71.3 (2008), 200–215.
- [25] D. Sol, S. Bacher, S. M. Reader, and L. Lefebvre. Brain size predicts the success of mammal species introduced into novel environments. *Am. nat.* 172.S1 (2008), S63–S71.
- [26] D. Sol. Revisiting the cognitive buffer hypothesis for the evolution of large brains. *Biol. lett.* 5.1 (2009), 130–133.
- [27] M. Grove. Speciation, diversity, and mode 1 technologies: the impact of variability selection. *J. hum. evol.* 61.3 (2011), 306–319.
- [28] A. Navarrete, C. P. van Schaik, and K. Isler. Energetics and the evolution of human brain size. *Nature* 480.7375 (2011), 91–93.

- [29] M. Will, M. Krapp, J. T. Stock, and A. Manica. Different environmental variables predict body and brain size evolution in homo. *Nat. commun.* 12.1 (2021), 4116.
- [30] J. M. Stibel. Climate change influences brain size in humans. *Brain behav. evol.* 98.2 (2023), 93–106.
- [31] A. Whiten and R. Byrne. The machiavellian intelligence hypotheses: editorial. in: byrne rw, whiten a, editors. *Machiavellian intelligence: social expertise and the evolution of intellect in monkeys, apes, and humans.* 413 (1988). Ed. by R. W. Byrne, 1–9.
- [32] R. I. M. Dunbar. The social brain hypothesis. *Evol anthropol* 6.5 (1998), 178–190.
- [33] L. Barrett, P. Henzi, and D. Rendall. Social brains, simple minds: does social complexity really require cognitive complexity? *Philos. trans. r. soc. lond. b biol. sci.* 362.1480 (2007), 561–575.
- [34] M. Grove and F. Coward. From individual neurons to social brains. *Camb. archaeol. j.* 18.3 (2008), 387–400.
- [35] C. Knight and C. Power. Social conditions for the evolutionary emergence of language. Oxford: Oxford University Press, 2011.
- [36] S. C. Hayes and B. T. Sanford. Cooperation came first: evolution and human cognition. *J. exp. anal. behav.* 101.1 (2014), 112–129.
- [37] R. I. M. Dunbar. The social brain hypothesis - thirty years on. *Ann. hum. biol.* 51.1 (2024), 2359920.
- [38] A. R. DeCasien, S. A. Williams, and J. P. Higham. Primate brain size is predicted by diet but not sociality. *Nat. ecol. evol.* 1.5 (2017), 112.
- [39] M. Grabowski, B. T. Kopperud, M. Tsuboi, and T. F. Hansen. Both diet and sociality affect primate brain-size evolution. *Syst. biol.* 72.2 (2023), 404–418.
- [40] M. A. Brockhurst, A. Buckling, and A. Gardner. Cooperation peaks at intermediate disturbance. *Curr. biol.* 17.9 (2007), 761–765.
- [41] S. Miller and J. Knowles. Population fluctuation promotes cooperation in networks. *Sci. rep.* 5 (2015), 11054.
- [42] C. S. Gokhale and C. Hauert. Eco-evolutionary dynamics of social dilemmas. *Theor. popul. biol.* 111 (2016), 28–42.
- [43] V. Stojkoski, M. Karbevski, Z. Utkovski, L. Basnarkov, and L. Kocarev. Evolution of cooperation in networked heterogeneous fluctuating environments. *Physica a* 572 (2021), 125904.
- [44] M. Assaf, M. Mobilia, and E. Roberts. Cooperation dilemma in finite populations under fluctuating environments. *Phys. rev. lett.* 111.23 (2013), 238101.

- [45] J. M. Borg and A. Channon. Testing the variability selection hypothesis: the adoption of social learning in increasingly variable environments. *International conference on the simulation and synthesis of living systems* (2012), 317–324.
- [46] M. Pereda, D. Zurro, J. I. Santos, I. Briz I Godino, M. Álvarez, J. Caro, et al. Emergence and evolution of cooperation under resource pressure. *Sci. rep.* 7 (2017), 45574.
- [47] M. Inaba and E. Akiyama. Environmental variability promotes the evolution of cooperation among geographically dispersed groups on dynamic networks. *Plos complex syst.* 2.4 (2025), e0000038.
- [48] C. K. W. De Dreu and Z. Triki. Intergroup conflict: origins, dynamics and consequences across taxa. *Philos. trans. r. soc. lond. b biol. sci.* 377.1851 (2022), 20210134.
- [49] A. M. M. Rodrigues, J. L. Barker, and E. J. H. Robinson. The evolution of intergroup cooperation. *Philos. trans. r. soc. lond. b biol. sci.* 378.1874 (2023), 20220074.
- [50] C. W. Marean. Pinnacle Point Cave 13B (Western Cape Province, South Africa) in context: the Cape floral kingdom, shellfish, and modern human origins. *J hum evol* 59.3-4 (2010), 425–443.
- [51] L. Wadley, C. Sievers, M. Bamford, P. Goldberg, F. Berna, and C. Miller. Middle stone age bedding construction and settlement patterns at Sibudu, South Africa. *Science* 334.6061 (2011), 1388–1391.
- [52] A. W. Kandel and N. J. Conard. Settlement patterns during the earlier and Middle stone age around Langebaan Lagoon, western Cape (South Africa). *Quat int* 270 (2012), 15–29.
- [53] K. Hasselmann. Stochastic climate models: Part I. Theory. *Tellus a* 28.6 (1976), 473–485.
- [54] D. Vyushin, P. Kushner, and F. Zwiers. Modeling and understanding persistence of climate variability. *J geophys res* 117.D21 (2012).
- [55] S. Salcedo-Sanz, D. Casillas-Pérez, J. Del Ser, C. Casanova-Mateo, L. Cuadra, M. Piles, et al. Persistence in complex systems. *Phys rep* 957 (2022), 1–73.
- [56] G. Hardin. The tragedy of the commons: the population problem has no technical solution; it requires a fundamental extension in morality. *Science* 162.3859 (1968), 1243–1248.
- [57] K. G. Binmore. Game theory and the social contract: just playing. Vol. 2. Cambridge: MIT Press, 1994.
- [58] P. Kollock. Social dilemmas: the anatomy of cooperation. *Annu. rev. sociol.* 24.1 (1998), 183–214.
- [59] F. C. Santos, M. D. Santos, and J. M. Pacheco. Social diversity promotes the emergence of cooperation in public goods games. *Nature* 454.7201 (2008), 213–216.
- [60] F. C. Santos and J. M. Pacheco. Scale-free networks provide a unifying framework for the emergence of cooperation. *Phys. rev. lett.* 95.9 (2005), 098104.

- [61] F. C. Santos, J. M. Pacheco, and T. Lenaerts. Evolutionary dynamics of social dilemmas in structured heterogeneous populations. *Proc. natl. acad. sci. u. s. a.* 103.9 (2006), 3490–3494.
- [62] Y. Meng, S. P. Cornelius, Y.-Y. Liu, and A. Li. Dynamics of collective cooperation under personalised strategy updates. *Nat. commun.* 15.1 (2024), 3125.
- [63] Z. Wang, L. Wang, A. Szolnoki, and M. Perc. Evolutionary games on multilayer networks: a colloquium. *Eur. phys. j. b* 88.5 (2015).
- [64] J. Gómez-Gardeñes, I. Reinares, A. Arenas, and L. M. Floría. Evolution of cooperation in multiplex networks. *Sci. rep.* 2 (2012), 620.
- [65] Q. Su, A. McAvoy, Y. Mori, and J. B. Plotkin. Evolution of prosocial behaviours in multilayer populations. *Nat. hum. behav.* 6.3 (2022), 338–348.
- [66] M. Inaba and E. Akiyama. Evolution of cooperation in multiplex networks through asymmetry between interaction and replacement. *Sci. rep.* 13.1 (2023), 9814.
- [67] P. Holme and J. Saramäki. Temporal networks. *Phys. rep.* 519.3 (2012), 97–125. DOI: [10.1016/j.physrep.2012.03.001](https://doi.org/10.1016/j.physrep.2012.03.001).
- [68] A. Li, L. Zhou, Q. Su, S. P. Cornelius, Y.-Y. Liu, L. Wang, et al. Evolution of cooperation on temporal networks. *Nat. commun.* 11.1 (2020), 2259.
- [69] N. Masuda and R. Lambiotte. A guide to temporal networks. World Scientific, 2020.
- [70] M. Inaba and E. Akiyama. Evolution of cooperation among migrating resource-oriented agents under environmental variability. *Arxiv* (2025).

# Acknowledgments